HHS Public Access

Author manuscript

J Med Chem. Author manuscript; available in PMC 2017 July 28.

Published in final edited form as:

J Med Chem. 2016 July 28; 59(14): 6826–6837. doi:10.1021/acs.jmedchem.6b00639.

Probing Lipophilic Adamantyl Group as the P1-Ligand for HIV-1 Protease Inhibitors: Design, Synthesis, Protein X-ray Structural Studies, and Biological Evaluation

Arun K. Ghosh[†,*], **Heather L. Osswald**[†], **Kristof Glauninger**[†], **Johnson Agniswamy**[‡], **Yuan-Fang Wang**[‡], **Hironori Hayashi**[≠,#], **Manabu Aoki**[≠,§,^], **Irene T. Weber**[‡], and **Hiroaki Mitsuya**[≠,#,§]

[†]Department of Chemistry and Department of Medicinal Chemistry, Purdue University, West Lafayette, IN 47907, USA

[‡]Department of Biology, Molecular Basis of Disease, Georgia State University, Atlanta, Georgia 30303, USA

[≠]Departments of Infectious Diseases and Hematology, Kumamoto University Graduate School of Biomedical Sciences, Kumamoto 860-8556, Japan

[^]Department of Medical Technology, Kumamoto Health Science University, Kumamoto 861-5598, Japan

[#]Center for Clinical Sciences, National Center for Global Health and Medicine, Tokyo 162-8655, Japan

[§]Experimental Retrovirology Section, HIV and AIDS Malignancy Branch, National Cancer Institute, National Institutes of Health, Bethesda, MD 20892, USA

Abstract

A series of potent HIV-1 protease inhibitors with a lipophilic adamantyl P1 ligand have been designed, synthesized and evaluated. We have developed an enantioselective synthesis of adamantane-derived hydroxyethylamine isostere utilizing Sharpless asymmetric epoxidation as the key step. Various inhibitors incorporating P1-adamanylmethyl in combination with P2-ligands such as 3-(*R*)-THF, 3-(*S*)-THF, bis-THF and THF-THP were examined. The S1′ pocket was also probed with phenyl and phenylmethyl ligands. Inhibitor **15d**, with an isobutyl P1′ ligand and a bis-THF P2 ligand proved to be the most potent of the series. The cLogP value of inhibitor **15d** is impoved compared to inhibitor **2** with a phenylmethyl P1-ligand. X-ray structural studies of **15d, 15h** and **15i** with HIV-1 protease complexes revealed molecular insight into the inhibitor-protein interaction.

[*]The corresponding author: Department of Chemistry and Department of Medicinal Chemistry, Purdue University, 560 Oval Drive, West Lafayette, IN 47907, Phone: (765)-494-5323; Fax: (765)-496-1612, akghosh@purdue.edu.

[†]The PDB accession codes for **15d, 15h** and **15i**-bound HIVP X-ray structures are: 5JFP, 5JFU and 5JG1

Supporting Information. This material is available free of charge via the Internet at http://pubs.acs.org." HPLC and HRMS data of inhibitors **15a–j** and crystallographic data collection, refinement statistics and electron density figures for inhibitors **15d, 15h,** and **15i**bound HIVP X-ray structures

Graphical Abstract

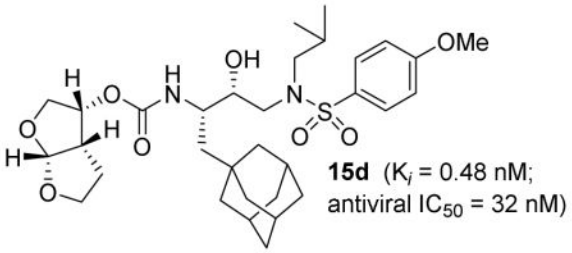

Keywords

Adamantane; HIV-1 protease inhibitors; antiviral; darunavir; multidrug-resistant; peptide isostere; synthesis; X-ray crystal structure; backbone binding

Introduction

The development of HIV-1 protease inhibitors (PIs) and their incorporation into antiretroviral therapy (ART) has dramatically reduced the mortality and morbidity rates of HIV/AIDS patients.[1–3] However, the growing emergence of drug-resistant strains of HIV has raised concerns as to the long-term viability of current treatment options.[4] In an effort to address this drug-resistance, our PI design strategy has been aimed at targeting the protease backbone, resulting in many potent inhibitors such as FDA approved darunavir, **1** (Figure 1) and related compound TMC-126, **2**.[5–8] The X-ray crystal structures of inhibitors **1**- and **2**-bound HIV-1 protease provided critical ligand-binding site interactions responsible for their broad-spectrum antiviral activity against multidrug-resistant HIV-1 variants.[9, 10]

In an effort to further optimize ligand-binding site interactions in the active site of HIV-1 protease, we have designed a stereochemically defined tris-tetrahydrofuran (tris-THF) as the P2 ligand.[8,11] The resulting inhibitor **3** exhibited significantly improved antiviral activity against a panel of multidrug-resistant HIV-1 variants compared to darunavir. An X-ray structure of inhibitor **3**-bound HIV-1 protease revealed that the ring oxygens of both A and B rings of tris-THF formed strong hydrogen bonds with the backbone atoms of Asp29 and Asp30 similar to darunavir.[12] However, the C-ring oxygen did not form any direct hydrogen bonds in the active site. Instead, it formed a water-mediated hydrogen bond with the side chain of Arg8′ in the active site.[11] Furthermore, it appeared that the ring C filled in the hydrophobic pocket in the S1 – S2 subsites. Based upon this specific ligand-binding site interaction, recently we have incorporated biphenyl rings to fill in the S1 – S2 extended subsite in the active site. Inhibitor **4** turned out to be a very potent inhibitor.[13] However, the X-ray structure of **4**-bound HIV-protease showed that the binding mode of the biphenyl ring was different than what we desired. The biphenyl ring rotated away from the S2 site and filled in a hydrophobic channel in the extended S1 subsite. Based upon this molecular insight, we further speculated that a bulkier, more uniform P1 ligand than biphenyl may maximize van der Waals interactions in S1 subsite. A number of other P1-ligand optimization attempts have been reported literature.[14,15] However, we are particularly interested in an adamantane-derived P1-ligand that can effectively fill in the hydrophobic

pocket as well as improve overall lipophilicity to improve drug properties.[16, 17] Indeed, an adamantane ring, regarded as a liphophilic bullet in medicinal chemistry, has been utilized in the design of numerous antiviral agents.[18] Also, an adamantane core is inherent to many approved therapeutics, such as amantadine[19], rimantadine[20], and tromantadine[21], which were among first marketed drugs. Herein, we report our studies on adamantane-derived protease inhibitors in inhibitor design, synthesis, biological evaluation, and X-ray structural studies of inhibitor-bound HIV-1 protease. A number of inhibitors displayed potent enzyme inhibitor activity. For our studies, we have developed an enantioselective synthesis of adamantane-derived hydroxyethylamine isosteres utilizing Sharpless asymmetric epoxidation as the key step.

Results and Discussion

The size and steric bulk of the adamantane group is quite different from the phenyl ring inherent to many potent protease inhibitors, including darunavir and TMC-126. It is possible that an optimized P2-ligand with a P1-phenylmethyl side chain may not be ideal for a P1-adamantanylmethyl side chain. To modulate ligand-binding site interactions in the S1 and S2 subsites, we plan to investigate P1-admentanylmethyl in combination with other P1′ and P2-ligands containing different steric, electronic, and stereochemical features. Adamantane-bearing dipeptide isosteres have not been previously reported. We, therefore, plan to devise an effective synthesis of hydroxyethylamine isosteres with an adamantanylmethyl group as a P1-ligand in an optically active form.

Our synthesis of adamantane-derived hydroxyethylamine sulfonamide isosteres is shown in Scheme 1. Commercially available 1-adamantaneethanol **5** was converted to the corresponding aldehyde by Swern oxidation.[22] Horner-Wadsworth-Emmons reaction of the resulting aldehyde with triethylphosphonoacetate and sodium hydride in THF at −78 °C to 23 °C provided α,β-unsaturated ester **6** in 74% yield. Reduction of this ester with Dibal-H in CH_2Cl_2 at 0 °C afforded allylic alcohol **7** in 80% yield. Sharpless asymmetric epoxidation of allylic alcohol **7** with (−)-diethyl-D-tartrate at −20 °C for 22 h furnished optically active epoxide **8** in excellent yield.[23] Epoxide **8** was subjected to azidotrimethylsilane and titanium isopropoxide in benzene at refluxing temperature as described by Sharpless and co-workers.[24] This has resulted in regioselective opening of epoxide **8**, providing azide diol **9** in 68% yield. The diol **9** was converted to epoxide **10** by exposure to 2-acetoxyisobutyryl chloride in $CHCl_3$ at 0 °C for 1 h. Treatment of the resulting chloroacetate with sodium methoxide in THF at 0 °C for 1 h provided epoxide **10** in 67% yield.[25]

For the synthesis of (*R*)-hydroxyethylamine sulfonamide isosteres, epoxide **10** was reacted with isobutylamine in DMF at 60 °C for 15 h to provide amine **11a** in 98% yield. As shown in Scheme 2, epoxide opeing with benzylamine under similar conditions afforded benzylamine derivative **11b** in 92% yield. Epoxide opening with aniline was carried out in the presence of lithium bromide and excess of aniline at 23 °C for 6 h as described in the literature.[26] This has provided amine **11c** in 84% yield. The secondary amines **11a–c** were then reacted with 4-methoxybenzenesulfonyl chloride or 4-nitrobenzenesulfonyl chloride in the presence of aqueous $NaHCO_3$ to furnish azidosulfonamide **12a–d**. These azide derivatives were reduced by catalytic hydrogenation over Pd/C under a hydrogen-filled

balloon in methanol to provide the amine derivatives **13a–d**.[27] This hydrogenation condition also reduced the aromatic nitro group in **12b** to the corresponding amine derivative.

For the synthesis of protease inhibitors containing P1 adamantanylmethyl group and varying P2-ligands, we planned to incorporate both enantiomers of 3-hydroxytetrahydrofuran and 3-hydroxy-bis-tetrahydrofuran as well as 3-hydroxyhexahydrofuropyran derivatives.[28] (Scheme 3) For the synthesis of respective carbamate derivative, the required activated carbonate derivatives of these ligands **14a–f** were prepared as described by us previously.[27, 28] Reaction of amine **13a** with succinimidyl carbonate **14a** in CH_3CN at 23 °C for 72 h in the presence of Et_3N afforded inhibitor **15a** in 56% yield. Similarly, other activated carbonate derivatives were reacted with amines **13a–d** to provide inhibitors **15b–j** in Table 1.

All inhibitors were evaluated in an enzyme inhibitory assay based on the protocol reported by Toth and Marshall.[29] Based on these results, selected inhibitors were further evaluated in antiviral assays. These results can be seen in Table 1. Inhibitors containing bis-THF as the P2 ligand (**15d**, **15e**, and **15f**) were more potent than derivatives with any other P2 ligand. This suggests that the expansion of hydrophobic contact and filling of the P1 pocket does not interfere with P2 ligand binding, despite their close proximity. It also indicates that the P1 adamantane group occupies the same space as the phenyl ring of darunavir **1** instead of the hydrophobic space closer to the P2 site that was occupied by the tris-THF containing inhibitor **3**. Inhibitors utilizing the (*S*)-THF P2 ligand from carbonate **14a** or (*R*)-bicyclic P2 ligands from carbonates **14c** and **14e** (inhibitors **15a**, **15d**, and **15i**) were more potent than derivatives with the enantiomeric P2 ligands (inhibitors **15b**, **15e**, and **15j**) which agrees with what has been previously shown in the literature. Analysis of the TMC-126 and darunavir derivatives, **15d** and **15f**, shows a shows a similar potency pattern, with the *p*-methoxybenzene sulfonamide P2′ isostere being more potent than the *p*-aminobenzene sulfonamide P2′ isostere in both enzymatic and antiviral assays with K_i values of 0.48 nM and 0.73 nM, respectively, and antiviral IC_{50} values of 32 nM and 60 nM, respectively. The cLogP value for inhibitor **15d** is 6.53 compared to cLogP value of 3.78 for inhibitor **2**, which indicates that adamantane-derived inhibitors may possibly improve membrane permeability significantly. When comparing P1′ ligands, isobutylamine remains to be preferred when paired with an adamantane P1 ligand. While both the phenylamine **15g** and benzylamine **15h** were potent inhibitors, with K_i values of 1.1 and 8.5 nM, respectively, both were less potent than the isobutylamine derivative, **15d** with a K_i value of 0.48 nM. However, the fold-change between enzymatic K_i and antiviral IC_{50} values is less for benzylamine derivative **15h**, 36-fold-change, than for isobutylamine derivative **15d**, 67-fold change. This suggests that while the potency is not necessarily better, the cell membrane permeability may be enhanced, allowing for more inhibitor to interact with the enzyme after cell membrane penetration. Furthermore, enzymatic activity trends show that activity decreases as the size of the P1′ ligand increases. This suggests that while the S1′ pocket may be able to accommodate larger moieties, the van der Waals contacts are optimal with isobutyl, which remains the preferred side chain in this series.

We selected inhibitors **15a** and **15d** for further evaluation against a panel of multidrug resistant (MDR) HIV-1 variants. The antiviral activity of these compounds were also

compared to clinically available PIs, darunavir (DRV) and amprenavir (APV).[9] The results are shown in Table 2. Inhibitor **15d** exhibited low nanomolar IC_{50} value comparable to APV against the wild-type HIV-1_{NL4-3}. Inhibitor **15d** also displayed comparable antiviral activity against viral strain C to APV. However, it did not show any appreciable antiviral activity against viral strains B and HIV-1 $_{DRV}{}^{R}{}_{20}$. Inhibitor **15a** was significantly less potent against the wild-type HIV-1_{NL4-3} and it did not exhibit appreciable antiviral activity against viral strains tested. DRV exhibited superior activity against the multi-drug resistant HIV-1 variants tested.

To gain insight into the inhibitor-enzyme interactions, the X-ray crystal structure of wild type **15d**-bound HIV protease was solved at 1.49 Å resolution with R_{work} and R_{free} values of 21.5 and 23.7%. A stereoview of the active site interactions is shown in Figure 2. The structure contains one protease dimer with inhibitor **15d** bound at the active site in a single conformation. The overall structure of the protease complex is comparable to the HIV-1 protease complex with darunavir[30] with root mean square difference of 0.33Å for 198 Cα atoms. The largest difference of 2.4 Å occurs at Pro81, indicating a shift in the position of the 80's loop. The bis-THF P2 ligand forms strong hydrogen bonding interactions with the backbone NH of Asp29 and Asp30 while the carbamate NH forms a hydrogen bond with the carbonyl oxygen of Gly27. The transition state hydroxyl group forms hydrogen bonds with the Asp25 and Asp25′ side chain carboxylates. The P2′ methoxy group hydrogen bonds to the backbone NH of Asp30′. A water-mediated hydrogen bonding network is formed between the NHs of Ile50 and Ile50′ to the conserved, structural water molecule which, in turn, hydrogen bonds to the P2 carbamate carbonyl and the P2′ sulfonamide. The salient feature of inhibitor **15d** is the adamantanylmethyl group in the P1 position. This bulky P1 group forms van der Waals interactions with 80's loop residues (Thr80, Pro81, Val82 and Ile84), flap residues (Gly48, Gly49 and Ile50) and Gly27 from the catalytic triad in the inhibitor-protease complex. The P1′-isobutyl group forms van der Waals contacts with Leu23′, Asp25′, Gly27 and Val82′.

An overlay of the X-ray crystal structures of inhibitors **2** (TMC-126) and **15d** in the HIV-1 protease active site is shown in Figure 3. As can be seen, the key interactions in the S2, S1′ and S2′ subsites are very similar. The major differences are in van der Waals interactions for **15d** are due to the adamantanylmethyl group vs the phenylmethyl group of inhibitor **2**. In particular, the key hydrogen bonding distances from the oxygens of the bis-THF moiety with the Asp29 and Asp30 backbone NHs were conserved with 2.9, 3.2, and 3.0 Å in **2** to 2.9, 3.2, and 3.1 Å in **15d**. The side view of Figure 3 shows protein surface interaction of both inhibitors. The adamantanylmethyl group occupies greater volume than that of the phenylmethyl group of inhibitor **2**. This does better fill the S1 pocket as predicted; however, the close proximity of the van der Waals radius of the inhibitor **15d** and enzyme atoms may destabilize the interaction as compared to that of **2**. The adamantyl group lies within 0.8 Å of the enzyme in the S1 pocket whereas **2** affords much more room with 1.6 Å between the benzyl group and the enzyme pocket. This effect may explain the difference of enzyme inhibitory and antiviral activity between these two inhibitors.

We have also determined the crystal structures of HIV-1 protease in complex with inhibitors **15h** and **15i** at 1.7 Å and 1.1 Å, respectively, and refined to R_{work}/R_{free} values of 22.8/27.8%

and 15.8/19.2%, respectively. Both crystal structures contain one protease dimer with an inhibitor bound at the active site in a single conformation. The active site interactions of inhibitor **15h** are shown in Figure 4. This inhibitor **15h** shows a similar binding pattern as the inhibitor **15d**, except in the S1′ subsite where the P1′ benzyl group occupies the hydrophobic pocket instead of the isobutyl in **15i** and **15d**. The bigger benzyl group in the S1′ subsite has contacts with Asp25′, Thr80′, Pro81′, and Ile84′, in addition to the flap residue Gly49.

The active site interactions of the X-ray crystal structure of **15i** and HIV-1 protease complex are shown in Figure 5. The inhibitor features an (*R*)-THF-THP P2 ligand and an adamantanylmethyl group as the P1 ligand. This inhibitor is significantly less active than inhibitor **15d**. The ligand-binding site interactions of inhibitor **15i** in the S1, S1′ and S2′ subsites are similar to inhibitor **15d**. However, the fused-tetrahydrofuranyltetrahydropyran rings in the S2 pocket, resulted in small alterations in hydrogen bond lengths and angles. These changes may be responsible for the decrease in potency of **15i** compared to **15d**. A comparison of hydrogen bonds for **15d** and **15i** with Asp29 and Asp30 NHs reveal that bond distances show little change, with bond lengths changing from 2.9, 3.2, and 3.1 Å in **15d** to 2.9, 3.4, and 3.1 Å in **15i**. However, there has been narrowing of bond angles for the (*R*)-THF-THP P2 ligand compared to bis-THF ligand in **15d**. The hydrogen bond angles and lengths appear to be more optimal for the bis-THF P2 ligand. These minor changes in the geometry of the hydrogen bonding interactions may explain the difference of activity between these two inhibitors.

Conclusions

We have designed, synthesized, and evaluated a series of inhibitors containing an adamantane moiety as the P1 ligand to improve hydrophobic contacts in the S1 site. An enantioselective adamantane-derived hydroxyethylamine isostere was synthesized utilizing Sharpless asymmetric epoxidation as the key step. A number of P2 ligands were examined including THF, bis-THF, and THF-THP in combination with P1-adamantyl ligand. Inhibitor **15d** proved to be the most potent. We have also examined (*R*)-THF-THP as the P2 ligand in combination with adamantanylmethyl group as the P1 ligand in inhibitor **15i**. The ligand contains one carbon atom more than the bis-THF ligand in darunavir. However, the inhibitor **15i** turns out be significantly less active than inhibitor **15d**. X-ray crystal structures of **15d, 15h,** and **15i** in the HIV-1 protease active site revealed extensive interactions of the bicyclic P2-ligands with the HIV-1 protease backbone atoms. However, the hydrophobic surface of the P1-adamantane ligand may be too close to the enzyme surface. The close 0.8 Å distance between the adamantyl P1 ligand and the S1 pocket of the enzyme is unfavorable, resulting in an nonoptimal van der Waals radius and destabilizing the inhibitor-protein interaction. The 1.6 Å distance between the benzyl group of previous inhibitors and the enzyme S1 pocket provides much more favorable interactions. Further design and synthesis of inhibitors using this insight is in progress.

Experimental

All moisture-sensitive reactions were carried out in oven-dried glassware under an argon atmosphere unless otherwise stated. Anhydrous solvents were obtained as follows: Diethyl ether and tetrahydrofuran were distilled from sodium metal/benzophenone under argon. Toluene and dichloromethane were distilled from calcium hydride under argon. All other solvents were reagent grade. Column chromatography was performed using Silicycle SiliaFlash F60 230–400 mesh silica gel. Thin-layer chromatography was carried out using EMD Millipore TLC silica gel 60 F_{254} plates. ^{1}H NMR and ^{13}C NMR spectra were recorded on a Varian INOVA300, Bruker ARX400, Bruker DRX500, or Bruker AV-III-500-HD. Low-resolution mass spectra were collected on a Waters 600 LCMS or by the Purdue University Campus-Wide Mass Spectrometry Center. High-resolution mass spectra were collected by the Purdue University Campus-Wide Mass Spectrometry Center. HPLC analysis and purification was done an on Agilent 1100 series instrument using a YMC Pack ODS-A column of 4.6 mm ID for analysis and either 10 mm ID or 20 mm ID for purification. The purity of all test compounds was determined by HPLC analysis to be ≥95% pure.

Ethyl (*E*)-4-((3*r*,5*r*,7*r*)-adamantan-1-yl)but-2-enoate (6)

A solution of oxalyl chloride (2.62 mL, 30.51 mmol, 1.1 eq) in dry DCM (115 mL) under argon was cooled to −78°C. A mixture of **5** (5.0 g, 27.73 mmol, 1 eq) and dimethyl sulfoxide (4.33 mL, 61.01 mmol, 2.2 eq) in dry DCM (20 mL) was added via cannula. The reaction was stirred at −78°C for 15 minutes. Triethylamine (19.34 mL, 138.65 mmol, 5 eq) was added and the reaction was warmed to room temperature and stirred for 2 hours. The reaction was quenched with water (60 mL) and extracted with DCM (3x60 mL). The combined organic layer was washed with 1 M HCl, water, $NaHCO_3$, and brine, dried over Na_2SO_4, and concentrated *in vacuo* to provide the crude aldehyde as a yellow liquid.

Sodium hydride (60% dispersion in mineral oil, 1.66 g, 41.6 mmol, 1.5 eq) was suspended in dry THF (115 mL) under argon and cooled to 0°C. Triethyl phosphonoacetate (8.25 mL, 41.6 mmol, 1.5 eq) was added dropwise. The mixture was cooled to −78°C and the crude aldehyde in dry THF (20 mL) was added via cannula. The reaction was warmed slowly to room temperature and stirred for 1 hour. The reaction was quenched with NH_4Cl (30 mL) and the THF was evaporated *in vacuo*. Water (30 mL) and ethyl acetate (60 mL) were added to the residue. The aqueous layer was extracted with ethyl acetate (3x60 mL). The combined organic layer was washed with brine, dried over Na_2SO_4, and concentrated *in vacuo*. The crude product was purified via column chromatography (30% ethyl acetate/hexanes) to afford **6** (5.10 g, 74% yield, 2 steps) as a clear liquid; ^{1}H NMR (400 MHz, $CDCl_3$): δ 6.92 (dt, J = 15.8, 7.9 Hz, 1H), 5.76 - 5.68 (m, 1H), 4.11 (q, J = 7.1 Hz, 2H), 1.91 – 1.86 (m, 5H), 1.63 (d, J = 115.Hz, 3H), 1.55 (d, J = 12.4 Hz, 3H), 1.44 (s, 6H), 1.21 (t, J = 7.1 Hz, 3H); ^{13}C NMR (100 MHz, $CDCl_3$) δ 166.32, 145.85, 123.30, 60.00, 47.16, 42.44, 36.88, 33.42, 28.65, 14.27; LRMS-ESI (*m/z*): 249 [*M* + H].

(*E*)-4-((3*r*,5*r*,7*r*)-Adamantan-1-yl)but-2-en-1-ol (7)

Ester **6** (5.10 g, 20.52 mmol, 1 eq) was dissolved in dry DCM (100 mL) under argon and cooled to 0°C. DIBAl-H (1 M in hexanes, 61.56 mL, 61.56 mmol, 3 eq) was added and the

reaction was warmed to room temperature. After 30 minutes, the reaction was quenched with water (10 mL) and 1 M NaOH (10 mL) was added. The reaction was stirred for 15 minutes and then magnesium sulfate was added and stirred for an additional 15 minutes. The reaction was filtered over celite and concentrated *in vacuo*. The crude product was purified via column chromatography (15% ethyl acetate/hexanes) to afford **7** (3.38 g, 80% yield) as a colorless liquid; ^{1}H NMR (400 MHz, $CDCl_3$) δ 5.69 (dt, *J* = 14.7, 7.3 Hz, 1H), 5.58 (dt, *J* = 15.2, 5.8 Hz, 1H), 5.28 (s, 1H), 4.08 (d, *J* = 5.8 Hz, 2H), 1.92 (s, 3H), 1.79 (d, *J* = 7.3 Hz, 2H), 1.68 (d, *J* = 12.0 Hz, 3H), 1.59 (d, *J* = 11.6 Hz, 3H), 1.45 (d, *J* = 2.2 Hz, 5H); ^{13}C NMR (100 MHz, $CDCl_3$) δ 131.32, 129.23, 63.94, 53.55, 47.36, 42.53, 37.21, 32.95, 28.83. LRMS-CI (*m/z*): 207 [*M* + H].

((2*R*,3*R*)-3-(((3*R*,5*R*,7*R*)-Adamantan-1-yl)methyl)oxiran-2-yl)methanol (8)

A two-necked flask was charged with 4Å molecular sieves, flame-dried, and cooled to room temperature. Under argon, dry dichloromethane (160 mL) was added followed by Ti(*i*PrO)$_4$ (390 μL, 1.31 mmol, 0.08 eq) and (−)-diethyl D-tartrate (170 μL, 0.98 mmol, 0.06 eq). The mixture is cooled to −20°C. *Tert*-butyl hydroperoxide solution (5.0 – 6.0 M in decane, 3.5 mL, 35.99 mmol, 2.2 eq) was added dropwise and the reaction was stirred at −20°C for 30 minutes. Allylic alcohol **7** was dissolved in dry dichloromethane and added dropwise via cannula. The reaction was stirred at −20°C for 18 hours. The reaction was warmed to 0°C and water (50 mL) was added. The mixture was stirred for 30 minutes at 0°C. 30% NaOH (15 mL) was added and the reaction was warmed to room temperature and stirred for 1 hour at room temperature. The reaction was filtered to remove molecular sieves. The aqueous phase was extracted with dichloromethane (3 × 25 mL). The combined organic phase was washed with brine, dried over sodium sulfate, and concentrated under reduced pressure. The crude product was purified via column chromatography (30% ethyl acetate/hexanes to 50% ethyl acetate/hexanes) to give **8** as a colorless liquid (2.70 g, 84% yield); $[\alpha]_D^{23}$ +21.07° (*c* 1.12 $CHCl_3$); ^{1}H NMR (400 MHz, $CDCl_3$) δ 3.86 (d, *J* = 12.6 Hz, 1 H), 3.55 (d, *J* = 12.6, 1H), 3.01 – 2.96 (m, 1H), 2.79 (dt, *J* = 4.8, 2.5 Hz, 1H), 2.69 (s, 1H), 1.92 (s, 3H), 1.67 (d, *J* = 12.0 Hz, 3H), 1.60 (d *J* = 12.1 Hz, 3H), 1.54 (d, *J* = 2.4 Hz, 6H) 1.35 – 1.21 (m, 2H); ^{13}C NMR (100 MHz, $CDCl_3$) δ 61.79, 58.59, 52.53, 46.32, 42.74, 36.98, 32.60, 28.59. LRMS-CI (*m/z*): 223 [*M* + H].

(2*S*,3*S*)-4-((1*s*,3*R*)-Adamantan-1-yl)-3-azidobutane-1,2-diol (9)

A solution of titanium isopropoxide (5.1 mL, 17.22 mmol, 1.5 eq) and azidotrimethylsilane (2.3 mL, 17.22 mmol, 1.5 eq) was refluxed in benzene (70 mL) for 2 hours under argon. Epoxide **8** (2.38g, 10.71 mmol, 1 eq) was dissolved in benzene (30 mL), added to the refluxing solution, and stirred at reflux for 30 min. The reaction was cooled to room temperature. 30 mL 5% H_2SO_4 was added and stirred for 1 hour at room temperature. The reaction was extracted with ethyl acetate (3 × 25 mL), washed with $NaHCO_3$ and brine, dried over sodium sulfate, and concentrated under reduced pressure. The crude product was purified via column chromatography (30% ethyl acetate/hexanes) to give **9** as a white solid (1.94g, 68% yield); $[\alpha]_D^{23}$ −9.75° (*c* 0.8 $CHCl_3$); ^{1}H NMR (400 MHz, $CDCl_3$) δ 3.74 (d, *J* = 4.8 Hz, 2H), 3.65 (q, *J* = 5.0 Hz, 1H), 3.52 (ddd, *J* = 7.9, 5.1, 2.4 Hz, 1H), 2.43 – 2.07 (m, 2H), 1.99 (s, 3H), 1.72 (d, *J* = 12.0 Hz, 3H), 1.64 (d *J* = 12.0 Hz, 3H), 1.55 (s, 6H), 1.38 –

1.23 (m, 2H); ^{13}C NMR (100 MHz, $CDCl_3$) δ 74.99, 63.05, 59.94, 44.31, 42.61, 37.03, 32.02, 28.69; LRMS-APCI (*m/z*): 238 [$M - N_2$].

(2*S*)-2-((1*S*)-2-((1*s*,3*R*)-Adamantan-1-yl)-1-azidoethyl)oxirane (10)

Diol **9** (1.61 g, 6.06 mmol, 1 eq) was dissolved in chloroform (30 mL) under argon and cooled to 0°C. 2-acetoxyisobutyryl chloride (1.2 mL, 8.49 mmol, 1.4 eq) was added and the reaction was stirred for 1 hour at 0°C. The reaction was quenched with aq. $NaHCO_3$ and extracted with chloroform. The combined organic layer was washed with brine, dried over sodium sulfate, and concentrated under reduced pressure to provide the crude chloroacetate as a clear liquid.

The crude chloroacetate was dissolved in THF under argon and cooled to 0°C. Solid sodium methoxide (490 mg, 9.09 mmol, 1.5 eq) was added and the reaction was stirred at 0°C for 1 hour. The reaction was quenched with aq. NH_4Cl and extracted with ethyl acetate. The combined organic layer was washed with brine, dried over sodium sulfate, and concentrated under reduced pressure. The crude product was purified via column chromatography (100% hexanes to 10% ethyl aceate/hexanes) to afford **10** as a colorless oil (1.26 g, 67% yield, two-steps); $[\alpha]_D^{23}$ −2.71° (*c* 1.4 $CHCl_3$); ^{1}H NMR (400 MHz, $CDCl_3$) δ 3.35 (ddd, *J* = 8.6, 5.3, 3.4 Hz, 1H), 2.94 (ddd, *J* = 5.3, 3.8, 2.6 Hz, 1H), 2.76 (qd, *J* = 4.9, 3.3 Hz, 2H), 1.94 (s, 3H), 1.69 (d, *J* = 12.0 Hz, 3H), 1.61 (d, *J* = 12.2 Hz, 3H), 1.54 – 1.51 (m, 6H), 1.37 – 1.28 (m, 2H); ^{13}C NMR (100 MHz, $CDCl_3$) δ 58.03, 54.27, 45.39, 45.17, 42.51, 36.89, 31.92, 28.59. LRMS-CI (*m/z*): 220 [$M - N_2$].

(2*R*,3*S*)-4-((1*s*,3*R*)-Adamantan-1-yl)-3-azido-1-(isobutylamino)butan-2-ol (11a)

Epoxide **10** (500 mg, 2.02 mmol, 1 eq) was dissolved in dimethylformamide (10 mL) under argon. Isobutylamine (1.0 mL, 10.11 mmol, 5 eq) was added and the reaction was heated to 60°C and stirred for 15 hours at 60°C. Upon completion, water was added (30 mL) and extracted with diethyl ether. The organic layer was washed with water (3 × 10 mL) to remove excess DMF and then washed with brine, dried over sodium sulfate, and concentrated under reduced pressure. The crude product was purified via column chromatography (30% ethyl acetate/hexanes to 50% ethyl acetate/hexanes) to afford **11a** as a colorless oil (637 mg, 98% yield); $[\alpha]_D^{23}$ −12.74° (*c* 0.95 $CHCl_3$); ^{1}H NMR (400 MHz, $CDCl_3$) δ 3.55 (dt, *J* = 8.6, 4.1 Hz, 1H), 3.49 – 3.43 (m, 1H), 2.93 (s, 1H), 2.86 (s, 1H), 2.74 – 2.61 (m, 3H), 2.42 – 2.39 (m, 2H), 1.95 (s, 3H), 1.69 (d, *J* = 10.0 Hz, 3H), 1.62 (d, *J* = 12.1 Hz, 3H), 1.52 (s, 6H), 1.28 – 1.14 (m, 3H), 0.89 (dd, *J* = 6.7, 1.6 Hz, 6H); ^{13}C NMR (100 MHz, $CDCl_3$) δ 72.56, 60.65, 57.72, 50.18, 44.07, 42.58, 37.03, 31.99, 28.68, 28.53, 20.61; LRMS-ESI (*m/z*): 321 [M + H].

(2*R*,3*S*)-4-((1*s*,3*R*)-Adamantan-1-yl)-3-azido-1-(benzylamino)butan-2-ol (11b)

Epoxide **10** (50 mg, 0.20 mmol, 1 eq) was dissolved in dimethylformamide (1 mL) under argon. Benzylamine (110 μL, 10.11 mmol, 5 eq) was added and the reaction was heated to 60°C and stirred for 12 hours at 60°C. Upon completion, water was added (3 mL) and extracted with diethyl ether. The organic layer was washed with water (3 × 5 mL) to remove excess DMF and then washed with brine, dried over sodium sulfate, and concentrated under reduced pressure. The crude product was purified via column chromatography (30% ethyl

acetate/hexanes to 50% ethyl acetate/hexanes) to afford **11b** as a colorless oil (65 mg, 92% yield); $[\alpha]_D^{23}$ −8.61° (*c* 0.72 $CHCl_3$); ^{1}H NMR (400 MHz, Chloroform-*d*) δ 7.32 (dq, *J* = 17.8, 9.7, 8.4 Hz, 5H), 3.87 – 3.76 (m, 2H), 3.59 (dt, *J* = 8.3, 4.1 Hz, 1H), 3.53 – 3.46 (m, 1H), 2.85 – 2.68 (m, 2H), 1.97 (s, 3H), 1.71 (d, *J* = 11.7 Hz, 3H), 1.64 (d, *J* = 11.9 Hz, 3H), 1.53 (s, 6H), 1.29 – 1.15 (m, 3H); ^{13}C NMR (101 MHz, $CDCl_3$) δ 139.87, 128.70, 128.24, 127.41, 72.81, 60.64, 53.87, 49.70, 44.15, 42.62, 37.06, 32.04, 28.71; LRMS-ESI (*m/z*): 335 [*M* + H].

(2*R*,3*S*)-4-((1*s*,3*R*)-Adamantan-1-yl)-3-azido-1-(phenylamino)butan-2-ol (11c)

Lithium bromide (6 mg, 5 mol%, 0.07 mmol) was added to a neat mixture of epoxide **10** (330 mg, 1.33 mmol, 1 eq) and aniline (120 μL, 1.33 mmol, 1eq) under argon. The reaction was stirred at room temperature for 6 hours. The reaction was quenched with water and extracted with diethyl ether. The combined organic layer was washed with brine, dried over sodium sulfate, and concentrated. The crude product was purified via column chromatography (10% ethyl acetate/hexanes to 30% ethyl acetate/hexanes) to afford **11c** as a yellow liquid (382 mg, 84% yield); $[\alpha]_D^{23}$ −14.79° (*c* 0.94 $CHCl_3$); ^{1}H NMR (400 MHz, $CDCl_3$) δ 7.22 (t, *J* = 7.9 Hz, 2H), 6.79 (t, *J* = 7.3 Hz, 1H), 6.68 (d, *J* = 7.8 Hz, 2H), 3.81 (dt, *J* = 8.0, 3.7 Hz, 1H), 3.56 (q, *J* = 5.2 Hz, 1H), 3.34 (dd, *J* = 13.2, 3.1 Hz, 1H), 3.18 (dd, *J* = 13.1, 8.8 Hz, 1H), 2.01 (s, 3H), 1.75 (d, *J* = 11.9 Hz, 3H), 1.67 (d, *J* = 11.7 Hz, 3H), 1.57 (s, 6H), 1.33 (d, *J* = 5.5 Hz, 2H); ^{13}C (100 MHz, $CDCl_3$) δ 148.03, 129.47, 118.57, 113.69, 73.58, 60.74, 46.06, 44.07, 42.56, 36.97, 31.98, 28.64; LRMS-ESI (*m/z*): 363 [*M* + Na].

N-((2*R*,3*S*)-4-((1*s*,3*R*)-Adamantan-1-yl)-3-azido-2-hydroxybutyl)-*N*-isobutyl-4-methoxybenzenesulfonamide (12a)

Amine **11a** (447 mg, 1.40 mmol, 1 eq) was dissolved in 1:1 dichloromethane/aq. sodium bicarbonate. 4-methoxybenzenesulfonyl chloride (318 mg, 1.54 mmol, 1.1eq) was added and the reaction was stirred overnight (20 hours). The reaction was diluted with dichloromethane and the phases were separated. The aqueous phase was extracted with dichloromethane. The combined organic phase was washed with brine, dried over sodium sulfate, and concentrated under reduced pressure. The crude product was purified via column chromatography (10% ethyl acetate/hexanes to 30% ethyl acetate/hexanes) to provide **12a** as a white solid (422 mg, 61% yield); $[\alpha]_D^{23}$ −27.17° (*c* 1.1 $CHCl_3$); ^{1}H NMR (400 MHz, $CDCl_3$) δ 7.75 (d, *J* = 8.8 Hz, 2H), 7.00 (d, *J* = 8.8 Hz), 3.87 (s, 3H), 3.77 (td, *J* = 5.7, 4.7, 2.2 Hz, 1H), 3.49 (d, *J* = 2.6 Hz, 1H), 3.44 (ddd, *J* = 8.5, 4.8, 1.6 Hz, 1H), 3.24 (dd, *J* = 15.3, 9.6 Hz, 1H), 3.06 – 2.93 (m, 2H), 2.88 – 2.78 (m, 1H), 1.97 (s, 3H), 1.85 (dt, *J* = 14.5, 6.6 Hz, 1H), 1.71 (d, *J* = 12.2 Hz, 3H), 1.63 (d, *J* = 11.8 Hz, 3H), 1.52 (s, 6H), 1.27 – 1.16 (m, 2H), 0.93 (dd, *J* = 22.3, 6.6, 6H); ^{13}C NMR (100 MHz, $CDCl_3$) δ 163.23, 129.92, 129.64, 114.52, 74.13, 60.73, 58.90, 55.77, 52.30, 44.20, 42.58, 37.00, 32.05, 28.66, 27.38, 20.34, 19.99; LRMS-ESI (*m/z*): 513 [*M* + Na].

N-((2*R*,3*S*)-4-((1*s*,3*R*)-Adamantan-1-yl)-3-azido-2-hydroxybutyl)-*N*-isobutyl-4-nitrobenzenesulfonamide (12b)

Amine **11a** (78 mg, 0.24 mmol, 1 eq) was dissolved in 1:1 dichloromethane/aq. sodium bicarbonate. 4-nitrobenzenesulfonyl chloride (59 mg, 0.27 mmol, 1.1eq) was added and the

reaction was stirred overnight (18 hours). The reaction was diluted with dichloromethane and the phases were separated. The aqueous phase was extracted with dichloromethane. The combined organic phase was washed with brine, dried over sodium sulfate, and concentrated under reduced pressure. The crude product was purified via column chromatography (10% ethyl acetate/hexanes to 30% ethyl acetate/hexanes) to provide **12b** as a white solid (67 mg, 55% yield); $[\alpha]_D^{23}$ −30.86° (*c* 1.1 $CHCl_3$); ^{1}H NMR (400 MHz, $CDCl_3$) δ 8.38 (d, *J* = 8.8 Hz, 2H), 8.01 (d, *J* = 8.8 Hz, 2H), 3.79 (dtd, *J* = 9.0, 4.4, 2.1 Hz, 1H), 3.45 (ddd, *J* = 7.2, 4.6, 2.3 Hz, 1H), 3.30 (dd, *J* = 15.3, 9.5 Hz, 1H), 3.08 (ddd, *J* = 15.5, 10.9, 5.1 Hz, 3H), 2.97 (dd, *J* = 13.5, 7.1 Hz, 1H), 1.97 (s, 3H), 1.90 (dt, *J* = 14.0, 7.0 Hz, 1H), 1.71 (d, *J* = 12.0 Hz, 3H), 1.62 (d, *J* = 11.9 Hz), 1.52 (s, 6H), 1.26 – 1.22 (m, 2H), 0.91 (dd, *J* = 18.1, 6.6 Hz, 6H); ^{13}C NMR (100 MHz, $CDCl_3$) δ 150.23, 144.71, 128.66, 124.54, 73.88, 60.88, 58.22, 51.76, 44.21, 42.55, 36.93, 32.01, 28.61, 27.17, 19.91; LRMS-ESI (*m/z*): 528 [*M* + Na].

N-((2*R*,3*S*)-4-((1*s*,3*R*)-Adamantan-1-yl)-3-azido-2-hydroxybutyl)-*N*-benzyl-4-methoxybenzenesulfonamide (12c)

Amine **11b** (65 mg, 0.18 mmol, 1 eq) was dissolved in 1:1 dichloromethane/aq. sodium bicarbonate. 4-methoxybenzenesulfonyl chloride (42 mg, 0.20 mmol, 1.1eq) was added and the reaction was stirred overnight (16 hours). The reaction was diluted with dichloromethane and the phases were separated. The aqueous phase was extracted with dichloromethane. The combined organic phase was washed with brine, dried over sodium sulfate, and concentrated under reduced pressure. The crude product was purified via column chromatography (10% ethyl acetate/hexanes to 30% ethyl acetate/hexanes) to provide **12c** as a white solid (88 mg, 94% yield); $[\alpha]_D^{23}$ −40.12° (*c* 0.82 $CHCl_3$); ^{1}H NMR (400 MHz, Chloroform-*d*) δ 7.81 (d, *J* = 8.9 Hz, 2H), 7.35 – 7.28 (m, 5H), 7.07 – 7.02 (m, 2H), 4.63 (d, *J* = 14.0 Hz, 1H), 4.01 (d, *J* = 14.0 Hz, 1H), 3.90 (s, 3H), 3.31 (d, *J* = 5.4 Hz, 2H), 3.26 (s, 2H), 2.97 (d, *J* = 14.2 Hz, 1H), 1.92 (s, 3H), 1.67 (d, *J* = 11.9 Hz, 3H), 1.57 (d, *J* = 10.6 Hz, 3H), 1.37 (d, *J* = 15.2 Hz, 6H), 0.87 (dd, *J* = 14.6, 8.4 Hz, 1H), 0.76 – 0.69 (m, 1H); ^{13}C NMR (101 MHz, $CDCl_3$) δ 187.91, 163.40, 135.75, 129.72, 129.10, 129.03, 114.70, 74.41, 60.54, 55.85, 54.77, 51.23, 43.99, 42.36, 36.98, 33.04, 31.88, 28.81, 28.60; LRMS-ESI (*m/z*): 547 [*M* + Na].

N-((2*R*,3*S*)-4-((1*s*,3*R*)-Adamantan-1-yl)-3-azido-2-hydroxybutyl)-4-methoxy-*N*-phenylbenzenesulfonamide (12d)

Amine **11b** (382 mg, 1.12 mmol, 1 eq) was dissolved in 1:1 dichloromethane/aq. sodium bicarbonate. 4-methoxybenzenesulfonyl chloride (254 mg, 1.23 mmol, 1.1eq) was added and the reaction was stirred overnight (18 hours). The reaction was diluted with dichloromethane and the phases were separated. The aqueous phase was extracted with dichloromethane. The combined organic phase was washed with brine, dried over sodium sulfate, and concentrated under reduced pressure. The crude product was purified via column chromatography (10% ethyl acetate/hexanes to 30% ethyl acetate/hexanes) to provide **12d** as a white solid (145 mg, 25% yield); $[\alpha]_D^{23}$ −5.62° (*c* 1.1 $CHCl_3$); ^{1}H NMR (400 MHz, Chloroform-*d*) δ 7.53 (d, *J* = 8.9 Hz, 2H), 7.38 – 7.29 (m, 3H), 7.13 – 7.05 (m, 2H), 6.94 (d, *J* = 8.9 Hz, 2H), 3.87 (s, 3H), 3.75 (dd, *J* = 14.0, 8.7 Hz, 1H), 3.62 (dd, *J* = 9.0, 4.9 Hz, 1H), 3.53 – 3.43 (m, 2H), 2.97 – 2.86 (m, 1H), 1.94 (s, 3H), 1.69 (d, *J* = 12.0 Hz, 3H), 1.60 (d, *J* = 11.7 Hz, 3H), 1.46 (s, 6H), 1.15 (d, *J* = 7.5 Hz, 2H); ^{13}C NMR (101 MHz, $CDCl_3$) δ 163.12, 139.65, 129.83, 129.25,

129.10, 128.63, 128.26, 114.03, 73.07, 59.87, 55.53, 53.57, 43.55, 42.28, 36.75, 31.71, 28.41. LRMS-ESI (*m/z*): 533 [*M* + Na].

N-((2*R*,3*S*)-4-((1*s*,3*R*)-Adamantan-1-yl)-3-amino-2-hydroxybutyl)-*N*-isobutyl-4-methoxybenzenesulfonamide (13a)

Azide **12a** (377 mg, 0.76 mmol, 1 eq) was dissolved in methanol (5 mL). The reaction vessel was flushed with argon. Palladium on carbon (10% Pd basis, 40 mg, 10 wt %) was added. The flask was evacuated and then subjected to a hydrogen atmosphere at 1 atm pressure. The reaction was allowed to stir at room temperature under a hydrogen atmostphere for 16 hours. The reaction was removed from hydrogen and celite (250 mg) was added. The methanol was evaporated under reduced pressure. Ethyl acetate was added and stirred for 30 min. The reaction was filtered, the celite pad was washed with ethyl acetate, and the solvent was evaporated under reduced pressure. The crude product was purified via column chromatography (5% methanol/dichloromethane – 10% methanol/dichloromethane) to afford **13a** as a white solid (198 mg, 38% yield); $[\alpha]_D^{23}$ −9.63° (*c* 0.81 $CHCl_3$); ^{1}H NMR (400 MHz, Chloroform-*d*) δ 7.75 (d, *J* = 8.7 Hz, 2H), 6.96 (d, *J* = 8.7 Hz, 2H), 3.85 (s, 3H), 3.66 (d, *J* = 8.2 Hz, 1H), 3.26 (dd, *J* = 15.0, 9.4 Hz, 1H), 3.15 – 3.11 (m, 1H), 3.02 – 2.83 (m, 7H), 1.94 (s, 3H), 1.68 (d, *J* = 11.6 Hz, 3H), 1.60 (d, *J* = 11.8 Hz, 3H), 1.53 (d, *J* = 11.5 Hz, 3H), 1.46 (d, *J* = 11.8 Hz, 3H), 1.25 – 1.17 (m, 1H), 1.03 – 0.97 (m, 1H), 0.90 (dd, *J* = 13.1, 6.6 Hz, 6H); ^{13}C NMR (101 MHz, $CDCl_3$) δ 162.98, 130.50, 129.61, 114.35, 74.25, 58.28, 55.71, 51.54, 49.62, 47.60, 42.95, 32.47, 28.65, 27.23, 20.30, 20.07; LRMS-ESI (*m/z*): 465 [*M* + H].

N-((2*R*,3*S*)-4-((1*s*,3*R*)-Adamantan-1-yl)-3-amino-2-hydroxybutyl)-4-amino-*N*-isobutylbenzenesulfonamide (13b)

Azide **12b** (67 mg, 0.13 mmol, 1 eq) was dissolved in methanol (1 mL). The reaction vessel was flushed with argon. Palladium on carbon (10% Pd basis, 7 mg, 10 wt %) was added. The flask was evaluated and then subjected to a hydrogen atmosphere at 1 atm pressure. The reaction was allowed to stir at room temperature under a hydrogen atmostphere for 20 hours. The reaction was removed from hydrogen and celite (100 mg) was added. The methanol was evaporated under reduced pressure. Ethyl acetate was added and stirred for 30 min. The reaction was filtered, the celite pad was washed with ethyl acetate, and the solvent was evaporated under reduced pressure. The crude product was purified via column chromatography (5% methanol/dichloromethane – 10% methanol/dichloromethane) to afford **13b** as a white solid (31 mg, 52% yield); ^{1}H NMR (500 MHz, Chloroform-*d*) δ 7.60 (d, *J* = 8.6 Hz, 2H), 6.69 (d, *J* = 8.6 Hz, 2H), 4.12 (s, 2H), 3.69 (d, *J* = 8.6 Hz, 1H), 3.36 – 3.25 (m, 1H), 3.21 – 3.15 (m, 1H), 2.99 (dd, *J* = 13.5, 8.0 Hz, 2H), 2.83 (dd, *J* = 13.4, 6.9 Hz, 1H), 1.96 (s, 3H), 1.90 (dd, *J* = 13.9, 6.9 Hz, 2H), 1.70 (d, *J* = 12.1 Hz, 3H), 1.62 (d, *J* = 11.3 Hz, 3H), 1.54 (d, *J* = 12.1 Hz, 3H), 1.47 (d, *J* = 11.7 Hz, 3H), 1.25 (s, 3H), 1.05 (dd, *J* = 14.4, 7.6 Hz, 1H), 0.92 (dd, *J* = 19.1, 6.6 Hz, 6H); ^{13}C NMR (126 MHz, $CDCl_3$) δ 150.66, 129.72, 126.96, 114.30, 58.56, 51.64, 49.80, 42.97, 37.05, 32.53, 29.85, 28.70, 27.36, 20.39, 20.12; LRMS-ESI (*m/z*): 450 [*M* + Na].

N-((2*R*,3*S*)-4-((1*s*,3*R*)-Adamantan-1-yl)-3-amino-2-hydroxybutyl)-*N*-benzyl-4-methoxybenzenesulfonamide (13c)

Azide **12c** (94 mg, 0.18 mmol, 1 eq) was dissolved in methanol (1 mL). The reaction vessel was flushed with argon. Palladium on carbon (10% Pd basis, 10 mg, 10 wt %) was added. The flask was evacuated and then subjected to a hydrogen atmosphere at 1 atmosphere pressure. The reaction was allowed to stir at room temperature under a hydrogen atmostphere for 16 hours. The reaction was removed from hydrogen and celite (100 mg) was added. The methanol was evaporated under reduced pressure. Ethyl acetate was added and stirred for 30 min. The reaction was filtered, the celite pad was washed with ethyl acetate, and the solvent was evaporated under reduced pressure. The crude product was purified via column chromatography (5% methanol/dichloromethane to 10% methanol/dichloromethane) to afford **13c** as a white solid (31 mg, 34% yield).

N-((2*R*,3*S*)-4-((1*s*,3*R*)-adamantan-1-yl)-3-amino-2-hydroxybutyl)-4-methoxy-*N*-phenylbenzenesulfonamide (13d)

Azide **12d** (94 mg, 0.18 mmol, 1 eq) was dissolved in methanol (1 mL). The reaction vessel was flushed with argon. Palladium on carbon (10% Pd basis, 10 mg, 10 wt %) was added. The flask was evacuated and then subjected to a hydrogen atmosphere at 1 atm pressure. The reaction was allowed to stir at room temperature under a hydrogen atmostphere for 16 hours. The reaction was removed from hydrogen and celite (100 mg) was added. The methanol was evaporated under reduced pressure. Ethyl acetate was added and stirred for 30 min. The reaction was filtered, the celite pad was washed with ethyl acetate, and the solvent was evaporated under reduced pressure. The crude product was purified via column chromatography (5% methanol/dichloromethane – 10% methanol/dichloromethane) to afford **13d** as a white solid (31 mg, 34% yield); $[\alpha]_D^{23}$ +10.78° (*c* 1.1 $CHCl_3$); ^{1}H NMR (400 MHz, Chloroform-*d*) δ 7.61 (d, *J* = 8.0 Hz, 2H), 7.26 (s, 3H), 7.07 (s, 2H), 6.90 (d, *J* = 7.8 Hz, 2H), 4.93 – 4.81 (m, 2H), 4.01 – 3.91 (m, 1H), 3.82 (s, 3H), 3.51 (s, 2H), 3.43 (s, 2H), 1.80 (s, 3H), 1.61 – 1.53 (m, 3H), 1.49 (s, 3H), 1.41 – 1.29 (m, 6H), 1.26 – 1.20 (m, 2H); ^{13}C NMR (101 MHz, $CDCl_3$) δ 163.19, 139.52, 130.27, 129.26, 129.15, 128.28, 114.21, 70.90, 55.69, 52.80, 50.66, 50.45, 43.48, 42.34, 36.69, 32.01, 28.47; LRMS-ESI (*m/z*): 485 [*M* + H].

(*S*)-Tetrahydrofuran-3-yl ((2*S*,3*R*)-1-((1*s*,3*R*)-adamantan-1-yl)-3-hydroxy-4-((*N*-isobutyl-4-methoxyphenyl)sulfonamido)butan-2-yl)carbamate (15a)

Amine **13a** (22 mg, 0.047 mmol, 1 eq) was dissolved in acetonitrile. Carbonate **14a** (11 mg, 0.047 mmol, 1 eq) and triethylamine (13 μL, 0.095 mmol, 2 eq) were added and the reaction was stirred at room temperature for 72 hours. The reaction was concentrated to afford the crude product. The crude product was purified via column chromatography (5% methanol/dichloromethane – 10% methanol/dichloromethane) to afford inhibitor **15a** as a white solid (15 mg, 56% yield); ^{1}H NMR (500 MHz, $CDCl_3$) δ 7.74 (d, *J* = 8.9 Hz, 2H), 6.99 (d, *J* = 8.8 Hz, 2H), 5.23 (s, 1H), 4.76 (d, *J* = 8.6 Hz, 1H), 3.91 (dd, *J* = 9.8, 6.2 Hz, 2H), 3.88 (s, 3H), 3.83 (td, *J* = 8.7, 4.6 Hz, 2H), 3.76 (dd, *J* = 18.4, 8.8 Hz, 2H), 3.64 (td, *J* = 8.6, 4.1 Hz, 1H), 3.39 – 3.33 (m, 1H), 3.12 (dd, *J* = 15.2, 9.1 Hz, 1H), 3.03 – 2.92 (m, 2H), 2.84 (dd, *J* = 13.4, 6.7 Hz, 1H), 2.14 (dq, *J* = 15.3, 8.8, 6.9 Hz, 1H), 2.01 – 1.97 (m, 1H), 1.94 (s, 3H), 1.88 (dt,

J = 1.5, 6.9 Hz, 1H), 1.69 (d, *J* = 12.1 Hz, 3H), 1.61 (d, *J* = 11.8 Hz, 3H), 1.51 (s, 3H), 1.48 – 1.41 (m, 4H), 0.93 – 0.88 (m, 6H); ^{13}C NMR (126 MHz, $CDCl_3$) δ 163.16, 155.82, 130.34, 129.67, 114.47, 77.41, 77.16, 76.91, 75.47, 74.30, 73.79, 67.16, 58.54, 55.78, 53.17, 50.22, 44.78, 42.74, 37.04z, 32.26, 29.86, 28.69, 27.32, 20.07; LRMS-ESI (*m/z*): 601 [*M* + Na]; HRMS-ESI (*m/z*) $[M + H]^+$ calculated for $C_{30}H_{46}N_2O_7S$ 579.3104, found 579.31235; 97.2% pure via HPLC analysis.

(*R*)-Tetrahydrofuran-3-yl ((2*S*,3*R*)-1-((1*s*,3*R*)-adamantan-1-yl)-3-hydroxy-4-((*N*-isobutyl-4-methoxyphenyl)sulfonamido)butan-2-yl)carbamate (15b)

Amine **13a** (8 mg, 0.017 mmol, 1 eq) was dissolved in acetonitrile. Carbonate **14b** (4 mg, 0.017 mmol, 1 eq) and triethylamine (5 μL, 0.034 mmol, 2 eq) were added and the reaction was stirred at room temperature for 60 hours. The reaction was concentrated to afford the crude product. The crude product was purified via column chromatography (5% methanol/dichloromethane – 10% methanol/dichloromethane) to afford inhibitor **15b** as a white solid (4 mg, 40% yield); ^{1}H NMR (500 MHz, Chloroform-*d*) δ 7.74 (d, *J* = 8.9 Hz, 2H), 7.00 (d, *J* = 8.9 Hz, 2H), 5.22 (s, 1H), 4.75 (d, *J* = 8.6 Hz, 1H), 3.88 (s, 3H), 3.84 (dt, *J* = 8.4, 4.2 Hz, 2H), 3.82 – 3.77 (m, 1H), 3.74 – 3.69 (m, 1H), 3.68 – 3.62 (m, 1H), 3.34 (d, *J* = 3.3 Hz, 1H), 3.10 (dd, *J* = 14.8, 8.6 Hz, 1H), 2.98 (dd, *J* = 13.4, 8.2 Hz, 2H), 2.85 (dd, *J* = 13.4, 6.9 Hz, 1H), 2.15 (dtd, *J* = 14.5, 8.7, 6.3 Hz, 1H), 1.98 (d, *J* = 6.1 Hz, 1H), 1.94 (s, 3H), 1.91 – 1.84 (m, 1H), 1.69 (d, *J* = 12.3 Hz, 3H), 1.61 (d, *J* = 11.8 Hz, 3H), 1.53 (d, *J* = 15.9 Hz, 5H), 1.46 (d, *J* = 10.3 Hz, 3H), 1.13 (dd, *J* = 14.9, 9.6 Hz, 1H), 0.91 (dd, *J* = 17.6, 6.6 Hz, 6H). ^{13}C NMR (125 MHz, $CDCl_3$) δ 163.15, 155.80, 130.26, 129.65, 114.47, 75.56, 74.32, 73.36, 67.11, 58.62, 55.78, 53.26, 50.30, 44.95, 42.76, 37.05, 33.29, 32.28, 28.71, 27.33, 20.32, 20.09; LRMS-ESI (*m/z*): 601 [*M* + Na]; HRMS-ESI (*m/z*) $[M + H]^+$ calculated for $C_{30}H_{46}N_2O_7S$ 579.3104, found 579.31175; 96.8% pure via HPLC analysis.

(*S*)-Tetrahydrofuran-3-yl ((2*S*,3*R*)-1-((1*s*,3*R*)-adamantan-1-yl)-4-((4-amino-*N*-isobutylphenyl) sulfonamido)-3-hydroxybutan-2-yl)carbamate (15c)

Amine **13b** (9 mg, 0.020 mmol, 1 eq) was dissolved in acetonitrile. Carbonate **14a** (5 mg, 0.020 mmol, 1 eq) and triethylamine (14 μL, 0.10 mmol, 5 eq) were added and the reaction was stirred at room temperature for 62 hours. The reaction was concentrated to afford the crude product. The crude product was purified via column chromatography (5% methanol/dichloromethane – 10% methanol/dichloromethane) to afford inhibitor **15c** as a white solid (5 mg, 45% yield); ^{1}H NMR (500 MHz, Chloroform-*d*) δ 7.56 (d, *J* = 8.6 Hz, 2H), 6.72 – 6.64 (m, 2H), 5.22 (s, 1H), 4.89 – 4.80 (m, 1H), 4.19 (s, 2H), 3.88 (dd, *J* = 10.6, 4.9 Hz, 2H), 3.82 (dt, *J* = 13.0, 6.8 Hz, 1H), 3.76 (d, *J* = 10.7 Hz, 1H), 3.75 – 3.70 (m, 1H), 3.63 (s, 1H), 3.45 (s, 1H), 3.09 (dd, *J* = 15.0, 9.2 Hz, 1H), 3.00 – 2.87 (m, 2H), 2.80 (dd, *J* = 13.2, 6.6 Hz, 1H), 2.13 (dq, *J* = 14.8, 7.8 Hz, 1H), 2.02 – 1.95 (m, 1H), 1.93 (s, 3H), 1.85 (dt, *J* = 13.1, 6.5 Hz, 1H), 1.68 (d, *J* = 11.5 Hz, 3H), 1.60 (d, *J* = 11.7 Hz, 3H), 1.51 (d, *J* = 11.8 Hz, 3H), 1.44 (d, *J* = 12.2 Hz, 3H), 1.39 (d, *J* = 15.1 Hz, 1H), 1.18 – 1.10 (m, 1H), 0.90 (dd, *J* = 21.9, 6.5 Hz, 6H); ^{13}C NMR (126 MHz, $CDCl_3$) δ 155.56, 150.69, 129.50, 126.43, 114.06, 76.77, 76.77, 75.22, 74.12, 73.62, 66.99, 58.47, 53.09, 49.98, 44.54, 42.56, 36.88, 32.79, 32.07, 28.53, 27.19, 20.20, 19.94; LRMS-ESI (*m/z*): 586 [*M* + Na]; HRMS-ESI (*m/z*) $[M + H]^+$ calculated for $C_{29}H_{45}N_3O_6S$ 579.3014, found 579.31235; 98.3% pure via HPLC analysis.

(3*R*,3a*S*,6a*R*)-Hexahydrofuro[2,3-*b*]furan-3-yl ((2*S*,3*R*)-1-((1*s*,3*R*)-adamantan-1-yl)-3-hydroxy-4-((*N*-isobutyl-4-methoxyphenyl)sulfonamido)butan-2-yl)carbamate (15d)

Amine **13a** (13 mg, 0.028 mmol, 1 eq) was dissolved in acetonitrile. Carbonate **14c** (8 mg, 0.028 mmol, 1 eq) and triethylamine (8 μL, 0.056 mmol, 2 eq) were added and the reaction was stirred at room temperature for 48 hours. The reaction was concentrated to afford the crude product. The crude product was purified via column chromatography (5% methanol/dichloromethane – 10% methanol/dichloromethane) to afford inhibitor **15d** as a white solid (10 mg, 59% yield); ^{1}H NMR (500 MHz, Chloroform-*d*) δ 7.73 (d, *J* = 8.8 Hz, 2H), 6.99 (d, *J* = 8.8 Hz, 2H), 5.70 (d, *J* = 5.2 Hz, 1H), 5.14 (q, *J* = 6.7 Hz, 1H), 4.95 (d, *J* = 9.0 Hz, 1H), 4.02 (dd, *J* = 9.5, 6.5 Hz, 1H), 3.95 (td, *J* = 8.2, 2.4 Hz, 1H), 3.87 (s, 3H), 3.75 (dd, *J* = 9.4, 6.6 Hz, 2H), 3.66 (td, *J* = 9.1, 4.1 Hz, 1H), 3.43 – 3.22 (m, 1H), 3.11 (dd, *J* = 15.1, 9.0 Hz, 1H), 3.08 – 3.01 (m, 1H), 3.00 – 2.90 (m, 2H), 2.83 (dd, *J* = 13.4, 6.8 Hz, 1H), 2.03 – 1.96 (m, 1H), 1.93 (s, 3H), 1.86 (dt, *J* = 13.1, 7.8 Hz, 2H), 1.69 (d, *J* = 12.0 Hz, 3H), 1.60 (d, *J* = 11.8 Hz, 3H), 1.52 (d, *J* = 11.5 Hz, 3H), 1.45 (d, *J* = 11.9 Hz, 3H), 1.39 (d, *J* = 15.2 Hz, 1H), 1.27 – 1.11 (m, 2H), 0.90 (dd, *J* = 19.6, 6.6 Hz, 6H); ^{13}C NMR (126 MHz, $CDCl_3$) δ 163.16, 155.19, 130.15, 129.61, 114.46, 109.42, 74.20, 73.54, 70.84, 69.63, 58.57, 55.77, 53.20, 50.32, 45.42, 44.49, 42.79, 36.99, 32.23, 28.66, 27.32, 25.91, 20.30, 20.07; LRMS-ESI (*m/z*): 643 [*M* + Na]; HRMS-ESI (*m/z*) [*M* + H]$^{+}$ calculated for $C_{32}H_{48}N_2O_8S$ 621.3210, found 621.32166; 95.3% pure via HPLC analysis.

(3*S*,3a*R*,6a*S*)-Hexahydrofuro[2,3-*b*]furan-3-yl ((2*S*,3*R*)-1-((1*s*,3*R*)-adamantan-1-yl)-3-hydroxy-4-((*N*-isobutyl-4-methoxyphenyl)sulfonamido)butan-2-yl)carbamate (15e)

Amine **13a** (20 mg, 0.043 mmol, 1 eq) was dissolved in acetonitrile. Carbonate **14d** (12 mg, 0.043 mmol, 1 eq) and triethylamine (12 μL, 0.086 mmol, 2 eq) were added and the reaction was stirred at room temperature for 52 hours. The reaction was concentrated to afford the crude product. The crude product was purified via column chromatography (5% methanol/dichloromethane – 10% methanol/dichloromethane) to afford inhibitor **15e** as a white solid (16 mg, 59% yield); ^{1}H NMR (500 MHz, Chloroform-*d*) δ 7.73 (d, *J* = 8.8 Hz, 2H), 6.99 (d, *J* = 8.7 Hz, 2H), 5.70 (d, *J* = 5.1 Hz, 1H), 5.14 (q, *J* = 6.9 Hz, 1H), 4.93 (t, *J* = 9.0 Hz, 1H), 4.04 (ddd, *J* = 16.4, 9.5, 6.4 Hz, 1H), 3.99 – 3.92 (m, 1H), 3.87 (s, 3H), 3.78 – 3.74 (m, 1H), 3.71 (dd, *J* = 9.6, 6.6 Hz, 1H), 3.66 (t, *J* = 8.8 Hz, 1H), 3.36 (dd, *J* = 35.2, 3.1 Hz, 1H), 3.12 (dt, *J* = 14.7, 7.4 Hz, 1H), 3.07 – 3.02 (m, 1H), 2.99 (dd, *J* = 14.0, 5.6 Hz, 1H), 2.96 – 2.89 (m, 1H), 2.85 – 2.79 (m, 1H), 2.06 – 1.99 (m, 1H), 1.93 (s, 3H), 1.88 – 1.82 (m, 2H), 1.69 (d, *J* = 12.4 Hz, 3H), 1.60 (d, *J* = 11.8 Hz, 3H), 1.51 (d, *J* = 10.3 Hz, 3H), 1.44 (t, *J* = 11.8 Hz, 3H), 1.39 – 1.33 (m, 1H), 1.25 – 1.11 (m, 2H), 0.90 (dd, *J* = 22.3, 6.5 Hz, 6H); ^{13}C NMR (126 MHz, $CDCl_3$) δ 163.16, 155.33, 130.23, 129.60, 114.46, 109.42, 74.20, 73.45, 71.20, 69.72, 58.56, 55.78, 53.09, 50.33, 45.30, 44.49, 42.71, 36.98, 32.21, 28.64, 27.32, 26.11, 20.31, 20.03; LRMS-ESI (*m/z*): 643 [*M* + Na]; HRMS-ESI (*m/z*) [*M* + H]$^{+}$ calculated for $C_{32}H_{48}N_2O_8S$ 621.3210, found 621.32200; 96.1% pure via HPLC analysis.

(3*R*,3a*S*,6a*R*)-Hexahydrofuro[2,3-*b*]furan-3-yl ((2*S*,3*R*)-1-((1*s*,3*R*)-adamantan-1-yl)-4-((4-amino-*N*-isobutylphenyl)sulfonamido)-3-hydroxybutan-2-yl)carbamate (15f)

Amine **13b** (10 mg, 0.022 mmol, 1 eq) was dissolved in acetonitrile. Carbonate **14c** (6 mg, 0.022 mmol, 1 eq) and triethylamine (39 μL, 0.28 mmol, 5 eq) were added and the reaction

was stirred at room temperature for 40 hours. The reaction was concentrated to afford the crude product. The crude product was purified via column chromatography (5% methanol/dichloromethane – 10% methanol/dichloromethane) to afford inhibitor **15f** as a white solid (8 mg, 62% yield); ^{1}H NMR (500 MHz, Chloroform-*d*) δ 7.59 – 7.54 (m, 2H), 6.69 (d, *J* = 8.7 Hz, 2H), 5.71 (d, *J* = 5.2 Hz, 1H), 5.14 (q, *J* = 6.6 Hz, 1H), 4.92 (d, *J* = 9.0 Hz, 1H), 4.16 (s, 2H), 4.03 (dd, *J* = 9.4, 6.4 Hz, 1H), 3.95 (td, *J* = 8.3, 2.5 Hz, 1H), 3.90 – 3.85 (m, 1H), 3.75 (dd, *J* = 9.4, 6.7 Hz, 2H), 3.66 (td, *J* = 9.0, 3.9 Hz, 1H), 3.36 (s, 1H), 3.13 – 3.02 (m, 2H), 2.95 (dd, *J* = 13.3, 8.3 Hz, 1H), 2.89 (dd, *J* = 15.1, 2.2 Hz, 1H), 2.80 (dd, *J* = 13.4, 6.8 Hz, 1H), 2.01 (ddd, *J* = 8.2, 5.7, 2.9 Hz, 1H), 1.94 (s, 3H), 1.89 – 1.80 (m, 2H), 1.69 (d, *J* = 12.1 Hz, 3H), 1.61 (d, *J* = 11.7 Hz, 3H), 1.53 (d, *J* = 11.5 Hz, 3H), 1.46 (d, *J* = 11.9 Hz, 3H), 1.41 (d, *J* = 15.0 Hz, 1H), 1.28 – 1.23 (m, 1H), 1.17 (dd, *J* = 14.9, 9.9 Hz, 1H), 0.90 (dd, *J* = 19.2, 6.6 Hz, 6H); ^{13}C NMR (126 MHz, $CDCl_3$) δ 154.99, 150.66, 129.52, 126.36, 114.08, 109.29, 74.06, 73.36, 70.71, 69.51, 58.60, 53.20, 50.13, 45.26, 44.39, 42.65, 36.86, 32.09, 28.53, 27.24, 25.77, 20.20, 19.95; LRMS-ESI (*m/z*): 628 [*M* + Na]; HRMS-ESI (*m/z*) [*M* + H]$^+$ calculated for $C_{31}H_{47}N_3O_7S$ 606.3213, found 606.32100; 95.4% pure via HPLC analysis.

(3*R*,3a*S*,6a*R*)-Hexahydrofuro[2,3-*b*]furan-3-yl ((2*S*,3*R*)-1-((1*s*,3*R*)-adamantan-1-yl)-3-hydroxy-4-((4-methoxy-*N*-phenylphenyl)sulfonamido)butan-2-yl)carbamate (15g)

Amine **13d** (20 mg, 0.041 mmol, 1 eq) was dissolved in acetonitrile. Carbonate **14c** (11 mg, 0.041 mmol, 1 eq) and triethylamine (12 μL, 0.083 mmol, 2 eq) were added and the reaction was stirred at room temperature for 58 hours. The reaction was concentrated to afford the crude product. The crude product was purified via column chromatography (5% methanol/dichloromethane – 10% methanol/dichloromethane) to afford inhibitor **15g** as a white solid (15 mg, 58% yield); ^{1}H NMR (500 MHz, Chloroform-*d*) δ 7.49 (d, *J* = 8.9 Hz, 2H), 7.32 (d, *J* = 6.4 Hz, 3H), 7.09 – 7.05 (m, 2H), 6.92 (d, *J* = 8.9 Hz, 2H), 5.70 (d, *J* = 5.1 Hz, 1H), 5.11 (q, *J* = 6.6 Hz, 1H), 4.98 (d, *J* = 9.0 Hz, 1H), 4.01 (dd, *J* = 9.5, 6.5 Hz, 1H), 3.95 (td, *J* = 8.4, 2.4 Hz, 1H), 3.87 (s, 3H), 3.80 – 3.71 (m, 2H), 3.57 (dd, *J* = 17.2, 8.9 Hz, 3H), 3.07 – 3.00 (m, 1H), 2.99 – 2.91 (m, 1H), 2.02 – 1.96 (m, 1H), 1.93 (s, 3H), 1.89 – 1.80 (m, 1H), 1.69 (d, *J* = 12.1 Hz, 3H), 1.60 (d, *J* = 11.8 Hz, 3H), 1.51 (d, *J* = 11.8 Hz, 3H), 1.45 (d, *J* = 12.1 Hz, 3H), 1.39 (d, *J* = 14.8 Hz, 1H), 1.32 – 1.24 (m, 2H); ^{13}C NMR (126 MHz, $CDCl_3$) δ 163.17, 155.40, 139.59, 129.87, 129.26, 129.17, 128.64, 128.24, 114.08, 109.29, 73.46, 73.40, 70.71, 69.52, 55.64, 53.84, 50.18, 45.26, 44.53, 42.59, 36.87, 32.17, 28.55, 25.81; LRMS-ESI (*m/z*): 663 [*M* + Na]; HRMS-ESI (*m/z*) [*M* + H]$^+$ calculated for $C_{34}H_{44}N_2O_8S$ 641.2897, found 641.29091; 97.3% purity via HPLC analysis.

(3*R*,3a*S*,6a*R*)-hexahydrofuro[2,3-*b*]furan-3-yl ((2*S*,3*R*)-1-((1*s*,3*R*)-adamantan-1-yl)-4-((*N*-benzyl-4-methoxyphenyl)sulfonamido)-3-hydroxybutan-2-yl)carbamate (15h)

Amine **13c** (13 mg, 0.026 mmol, 1 eq) was dissolved in acetonitrile. Carbonate **14c** (7 mg, 0.026 mmol, 1 eq) and triethylamine (8 μL, 0.060 mmol, 2 eq) were added and the reaction was stirred at room temperature for 48 hours. The reaction was concentrated to afford the crude product. The crude product was purified via column chromatography (5% methanol/dichloromethane – 10% methanol/dichloromethane) to afford inhibitor **15h** as a white solid (16 mg, 80% yield); ^{1}H NMR (500 MHz, Chloroform-*d*) δ 7.78 (d, *J* = 8.9 Hz, 2H), 7.32 (q, *J* = 7.8, 6.9 Hz, 3H), 7.27 (s, 2H), 7.01 (d, *J* = 8.8 Hz, 2H), 5.71 (d, *J* = 5.2 Hz, 1H), 5.10 (p,

J = 6.4 Hz, 1H), 4.63 (d, *J* = 8.9 Hz, 1H), 4.42 – 4.26 (m, 2H), 4.02 (dd, *J* = 9.6, 6.3 Hz, 1H), 3.94 (td, *J* = 8.2, 2.4 Hz, 1H), 3.89 (s, 3H), 3.88 – 3.81 (m, 1H), 3.73 (dd, *J* = 9.5, 6.6 Hz, 1H), 3.57 – 3.50 (m, 1H), 3.41 (d, *J* = 5.6 Hz, 1H), 3.09 – 3.01 (m, 3H), 1.96 (ddt, *J* = 10.3, 5.1, 2.4 Hz, 1H), 1.92 – 1.88 (m, 3H), 1.83 (ddd, *J* = 12.9, 7.4, 1.8 Hz, 1H), 1.67 (d, *J* = 11.9 Hz, 3H), 1.58 (s, 3H), 1.44 – 1.40 (m, 3H), 1.35 (d, *J* = 12.0 Hz, 3H), 1.26 (s, 1H), 0.90 – 0.86 (m, 2H); MR (126 MHz, $CDCl_3$) δ 163.29, 155.36, 136.01, 130.37, 129.66, 128.98, 128.33, 114.61, 109.43, 73.91, 73.56, 70.86, 69.65, 55.83, 54.03, 51.71, 50.24, 45.39, 44.67, 42.62, 36.98, 32.20, 29.85, 28.64, 25.92, 22.85; LRMS-ESI (*m/z*): 677 [*M* + Na]; HRMS-ESI (*m/z*) $[M + H]^+$ calculated for $C_{35}H_{46}N_2O_8S$ 655.3054, found 655.30729; 96.5% purity via HPLC analysis.

(3*R*,3a*S*,7a*R*)-hexahydro-4*H*-furo[2,3-*b*]pyran-3-yl ((2*S*,3*R*)-1-((1*s*,3*R*)-adamantan-1-yl)-3-hydroxy-4-((*N*-isobutyl-4-methoxyphenyl)sulfonamido)butan-2-yl)carbamate (15i)

Amine **13a** (20 mg, 0.049 mmol, 1 eq) was dissolved in acetonitrile. Carbonate **14e** (14 mg, 0.049 mmol, 1 eq) and triethylamine (14 μL, 0.098 mmol, 2 eq) were added and the reaction was stirred at room temperature for 42 hours. The reaction was concentrated to afford the crude product. The crude product was purified via column chromatography (5% methanol/dichloromethane – 10% methanol/dichloromethane) to afford inhibitor **15i** as a white solid (10 mg, 32% yield); ^{1}H NMR (500 MHz, Chloroform-*d*) δ 7.74 (d, *J* = 8.8 Hz, 2H), 7.00 (d, *J* = 8.9 Hz, 2H), 5.35 (td, *J* = 6.8, 3.7 Hz, 1H), 5.08 (d, *J* = 3.9 Hz, 1H), 4.89 (d, *J* = 8.8 Hz, 1H), 4.22 (dd, *J* = 10.0, 6.6 Hz, 1H), 3.99 (dd, *J* = 10.1, 3.5 Hz, 1H), 3.92 (d, *J* = 11.6 Hz, 1H), 3.88 (s, 3H), 3.77 – 3.71 (m, 1H), 3.67 (dd, *J* = 9.1, 4.4 Hz, 1H), 3.51 – 3.44 (m, 1H), 3.30 (s, 1H), 3.09 (dd, *J* = 15.1, 9.0 Hz, 2H), 2.99 – 2.93 (m, 2H), 2.85 (dd, *J* = 13.4, 6.9 Hz, 1H), 2.21 (dt, *J* = 6.7, 3.3 Hz, 1H), 1.93 (s, 3H), 1.87 (dd, *J* = 13.7, 7.7 Hz, 2H), 1.69 (d, *J* = 11.8 Hz, 3H), 1.61 (d, *J* = 11.6 Hz, 3H), 1.53 (d, *J* = 11.7 Hz, 3H), 1.47 (d, *J* = 14.6 Hz, 3H), 1.42 (s, 1H), 1.38 (dd, *J* = 9.7, 5.1 Hz, 1H), 1.16 (dd, *J* = 14.9, 9.3 Hz, 2H), 0.91 (dd, *J* = 16.9, 6.6 Hz, 6H); ^{13}C NMR (126 MHz, $CDCl_3$) δ 163.16, 155.78, 130.19, 129.66, 114.48, 101.35, 74.50, 74.28, 73.08, 63.86, 58.62, 55.79, 53.27, 50.36, 44.78, 42.81, 39.86, 37.04, 32.26, 28.72, 27.33, 22.60, 20.32, 20.10; LRMS-ESI (*m/z*): 657 [*M* + Na]; HRMS-ESI (*m/z*) $[M + H]^+$ calculated for $C_{33}H_{50}N_2O_8S$ 635.3367, found 635.33882; 97.1% purity via HPLC analysis.

(3*S*,3a*R*,7a*S*)-hexahydro-4*H*-furo[2,3-*b*]pyran-3-yl ((2*S*,3*R*)-1-((1*s*,3*R*)-adamantan-1-yl)-3-hydroxy-4-((*N*-isobutyl-4-methoxyphenyl)sulfonamido)butan-2-yl)carbamate (15j)

Amine **13a** (20 mg, 0.049 mmol, 1 eq) was dissolved in acetonitrile. Carbonate **14f** (14 mg, 0.049 mmol, 1 eq) and triethylamine (14 μL, 0.098 mmol, 2 eq) were added and the reaction was stirred at room temperature for 44 hours. The reaction was concentrated to afford the crude product. The crude product was purified via column chromatography (5% methanol/dichloromethane – 10% methanol/dichloromethane) to afford inhibitor **15j** as a white solid (12 mg, 39% yield); ^{1}H NMR (500 MHz, Chloroform-*d*) δ 7.74 (d, *J* = 8.8 Hz, 2H), 6.99 (d, *J* = 8.7 Hz, 2H), 5.36 – 5.31 (m, 1H), 5.08 (d, *J* = 3.8 Hz, 1H), 4.87 (d, *J* = 8.6 Hz, 1H), 4.23 (dd, *J* = 10.0, 6.4 Hz, 1H), 4.00 – 3.95 (m, 1H), 3.92 (d, *J* = 11.5 Hz, 1H), 3.87 (s, 3H), 3.77 – 3.72 (m, 1H), 3.66 (td, *J* = 8.9, 4.2 Hz, 1H), 3.48 (t, *J* = 10.5 Hz, 1H), 3.40 (s, 1H), 3.32 – 3.27 (m, 1H), 3.15 – 3.08 (m, 1H), 2.98 (dq, *J* = 21.1, 7.2, 6.0 Hz, 2H), 2.87 – 2.79 (m, 2H), 2.23 – 2.18 (m, 1H), 1.94 (s, 3H), 1.88 (d, *J* = 7.7 Hz, 1H), 1.68 (s, 3H), 1.61 (d, *J* = 11.6 Hz,

3H), 1.51 (d, J = 10.2 Hz, 3H), 1.44 (d, J = 13.1 Hz, 3H), 1.38 (s, 1H), 1.25 (s, 1H), 1.19 – 1.12 (m, 2H), 0.93 – 0.87 (m, 6H); ^{13}C NMR (126 MHz, $CDCl_3$) δ 163.14, 155.96, 130.34, 129.61, 114.46, 109.84, 101.29, 74.59, 74.27, 73.20, 63.77, 58.62, 55.78, 53.08, 50.36, 44.63, 42.70, 39.78, 37.01, 32.25, 28.67, 27.34, 25.66, 22.60, 20.32; LRMS-ESI (m/z): 657 [M + Na]; HRMS-ESI (m/z) [M + H]$^+$ calculated for $C_{33}H_{50}N_2O_8S$ 635.3367, found 635.33875; 98.4% pure via HPLC analysis.

Methods: Determination of X-ray structures of HIV-1 protease-inhibitor complexes

The optimized HIV-1 protease was expressed and purified as described before.[31] The protease and inhibitor were mixed in a molar ratio of 1:5 and incubated on ice for 15 mins. The protease complexes with **15d**, **15h** and **15i** were crystallized by the hanging drop vapor diffusion technique with well solutions of 1.7 M NaCl, 1.15M LiCl, and 1.25 M NaCl, respectively, in 0.1 M Sodium Acetate buffer at pH 5.5. Diffraction data were collected on a single crystal of each complex cryo-cooled to 90 K at SER-CAT (22-ID and 22-BM beamlines), Advanced Photon Source, Argonne National Lab (Chicago, USA). The X-ray data were integrated and scaled using HKL-2000[32] with Rmerge values of 9.7%, 7.6% and 9.8%, respectively. The three structures were solved by molecular replacement using PHASER[33] in CCP4i Suite[34,35] with the previously solved HIV-1 protease-amprenavir complex (3NU3) as the starting model.[36] The structures were refined to a resolution of 1.49 Å, 1.7 Å and 1.16 Å, respectively, with SHELX-2014.[37] COOT[38] was used for manual rebuilding. PRODRG-2[39] was used to construct the inhibitor and the restraints for refinement. Visible alternate conformations were modeled and solvent molecules were inserted at stereo chemically reasonable positions. The final refined structure comprised one sodium ion, two chloride ions, 143 water molecules for the protease complex with **15d**, two chloride ions, 94 water molecules for **15h**, and three sodium ions, two chloride ions, one glycerol, 188 water molecules for the **15i** complex. The crystallographic statistics are listed in Table 1 (supporting information). The coordinates and structure factors of the HIVP complexes with **15d**, **15h** and **15i** were deposited in the Protein Data Bank[40] with accession codes of 5JFP, 5JFU and 5JG1.

Supplementary Material

Refer to Web version on PubMed Central for supplementary material.

Acknowledgments

This research was supported by the National Institutes of Health (Grant GM53386, AKG and Grant GM 62920, IW). X-ray data were collected at the Southeast Regional Collaborative Access Team (SER-CAT) beamline 22BM at the Advanced Photon Source, Argonne National Laboratory. Use of the Advanced Photon Source was supported by the US Department of Energy, Basic Energy Sciences, Office of Science, under Contract No. W-31-109-Eng-38. This work was also supported by the Intramural Research Program of the Center for Cancer Research, National Cancer Institute, National Institutes of Health, and in part by a Grant-in-Aid for Scientific Research (Priority Areas) from the Ministry of Education, Culture, Sports, Science, and Technology of Japan (Monbu Kagakusho), a Grant for Promotion of AIDS Research from the Ministry of Health, Welfare, and Labor of Japan, and the Grant to the Cooperative Research Project on Clinical and Epidemiological Studies of Emerging and Reemerging Infectious Diseases (Renkei Jigyo) of Monbu-Kagakusho. The authors would like to thank the Purdue University Center for Cancer Research, which supports the shared NMR and mass spectrometry facilities.

ABBREVIATIONS

THF	tetrahydrofuran
bis-THF	bis-tetrahydrofuran
THF-THP	tetrahydrofuran-tetrahydropyran
tris-THF	tris-tetrahydrofuran
PI	protease inhibitor
DMF	dimethylformamide
DIBALH	diisobutylaluminum hydride
HIV	human immunodeficiency virus
FDA	Food and Drug Administration
IC_{50}	half-maximum inhibitory concentration
K_i	inhibition constant
cLogP	calculated logarithm of partition coefficient

References

1. Montaner JSG, Lima VD, Barrios R, Yip B, Wood E, Kerr T, Shannon K, Harrigan PR, Hogg RS, Daly P, Kendall P. Association of highly active antiretroviral therapy coverage, population viral load, and yearly new HIV diagnoses in British Columbia, Canada: a population-based study. Lancet. 2010; 376:532–539. [PubMed: 20638713]
2. Braitstein P, Brinkhof MWG, Dabis F, Schechter M, Boulle A, Miotti P, Wood R, Laurent C, Sprinz E, Seyler C, Bangsberg DR, Balestre E, Sterne JAC, May M, Egger M. Mortality of HIV-1-infected patients in the first year of antiretroviral therapy: comparison between low-income and high-income countries. Lancet. 2006; 367:817–824. [PubMed: 16530575]
3. Esté JA, Cihlar T. Current status and challenges of antiretroviral research and therapy. Antiviral Res. 2010; 85:25–33. [PubMed: 20018390]
4. Waters L, Nelson M. Why do patients fail HIV therapy? Int J Clin Prac. 2007; 61:983–990.
5. Ghosh AK, Anderson DD, Weber IT, Mitsuya H. Enhancing backbond binding – a fruitful concept for combating drug-resistant HIV. Angew Chem Int Ed Engl. 2012; 51:1778–1802. [PubMed: 22290878]
6. Ghosh, AK., Chapsal, BD. Second-generation approved HIV protease inhibitors for the treatment of HIV/AIDS. In: Ghosh, AK., editor. Aspartic Acid Proteases as Therapeutic Targets. Wiley-VCH; Weinheim, Germany: 2010. p. 169-204.
7. Ghosh AK, Dawson ZL, Mitsuya H. Darunavir, a conceptually new HIV-1 protease inhibitor for the treatment of drug-resistant HIV. Bioorg Med Chem. 2007; 15:7576–7580. [PubMed: 17900913]
8. Amano M, Tojo Y, Salcedo-Gómez PM, Campbell JR, Das D, Aoki M, Xu CX, Rao KV, Ghosh AK, Mitsuya H. GRL-0519, a novel oxatricyclic ligand-containing nonpeptidic HIV-1 protease inhibitor (PI), potently suppresses replication of a wide spectrum of multi-PI-resistant HIV-1 variants in vitro. Antimicrob Agents Chemother. 2013; 57:2036–2046. [PubMed: 23403426]
9. Koh Y, Nakata H, Maeda K, Ogata H, Bilcer G, Devasamudram T, Kincaid JF, Boross P, Wang YF, Tie Y, Volarath P, Gaddis L, Harrison RW, Weber IT, Ghosh AK, Mitsuya H. Novel bis-tetrahydrofuranylurethane-containing nonpeptidic protease inhibitor (PI) UIC-94017 (TMC114)

with potent activity against multi-PI-resistant human immunodeficiency virus in vitro. Antimicrob Agents Chemother. 2003; 47:3123–3129. [PubMed: 14506019]

10. De Meyer S, Azijn H, Surleraux D, Jochmans D, Tahri A, Pauwels R, Wigerinck P, de Béthune MP. TMC114, a novel human immunodeficiency virus type 1 protease inhibitor active against protease-resistant viruses, including a broad range of clinical isolates. Antimicrob Agents Chemother. 2005; 49:2314–2321. [PubMed: 15917527]
11. Ghosh AK, Xu CX, Rao KV, Baldridge A, Agniswamy J, Want YF, Weber IT, Aoki M, Miguel SG, Amano M, Mitsuya H. Probing multidrug-resistance and protein-ligand interactions with oxatricyclic designed ligands in HIV-1 protease inhibitors. Chem Med Chem. 2010; 5:1850–1854. [PubMed: 20827746]
12. Zhang H, Wang YF, Shen CH, Agniswamy J, Rao KV, Xu CX, Ghosh AK, Harrison RW, Weber IT. Novel P2 tri-tetrahydrofuran group in antiviral compound 1 (GRL-0519) fills the S2 binding pocket of selected mutants of HIV-1 protease. J Med Chem. 2013; 56:1074–1083. [PubMed: 23298236]
13. Ghosh AK, Yu X, Osswald HL, Agniswamy J, Wang YF, Amano M, Weber IT, Mitsuya H. Structure-based design of potent HIV-1 protease inhibitors with modified P1-biphenyl ligands: synthesis, biological evaluation, and enzyme-inhibitor X-ray structural studies. J Med Chem. 2015; 58:5334–5343. [PubMed: 26107245]
14. Ghosh AK, Osswald HL, Prato G. Recent progress in the development of HIV-1 protease inhibitors for the treatment of HIV/AIDS. J Med Chem. Online early access. Published Online: January 22, 2016.
15. Motwani HV, De Rosa M, Odell LR, Hallberg A, Larhed M. Aspartic protease inhibitors containing tertiary alcohol transition-state mimics. Eur J Med Chem. 2015; 90:462–490. [PubMed: 25481814]
16. Chew CF, Guy A, Biggin PC. Distribution and dynamics of adamantanes in a lipid bilayer. Biophys J. 2008; 95:5627–5636. [PubMed: 18835906]
17. Danielczyk W. Twenty-five years of amantadine therapy in Parkinson's disease. J Neural Transm Suppl. 1995; 46:399–405. [PubMed: 8821075]
18. Wanka L, Iqbal K, Schreiner PR. The lipophilic bullet hits the targets: medicinal chemistry of adamantine derivatives. Chem Rev. 2013; 113:3516–3604. [PubMed: 23432396]
19. Davies WL, Grunert RR, Haff RF, McGahen JW, Neumayer EM, Paulshock M, Watts JC, Wood TR, Hermann EC, Hoffamnn CE. Antiviral activity of 1-adamantanamine (amantadine). Science. 1964; 144:862–863. [PubMed: 14151624]
20. Tsunoda A, Maassab HF, Cochran KW, Eveland WC. Antiviral activity of alpha-methyl-1-adamantanemethylamine hydrochloride. Antimicrob Agents Chemother. 1965; 5:553–560. [PubMed: 5883472]
21. Rosenthal KS, Sokol MS, Ingram RL, Subramanian R, Fort RC. Tromantadine: inhibitor of early and late events in herpes simplex virus replication. Antimicrob Agents Chemother. 1982; 22:1031–1036. [PubMed: 6297383]
22. Luly JR, Dellaria JF, Plattner JJ, Soderquist JL, Yi N. A synthesis of protected aminoalkyl epoxides from alpha-amino acids. J Org Chem. 1987; 52:1487–1492.
23. Katsuki T, Sharpless KB. The first practical method for asymmetric epoxidation. J Am Chem Soc. 1980; 102:5974–5976.
24. Caron M, Carlier PR, Sharpless KB. Regioselective azide opening of 2,3-epoxy alcohols by [Ti(O-i-Pr)2(N3)2]: synthesis of alpha-amino acids. J Org Chem. 1988; 53:5185–5187.
25. Ghosh AK, Swanson LM, Cho H, Leshchenko S, Hussain KA, Kay S, Walters DE, Koh Y, Mitsuya H. Structure-based design: synthesis and biological evaluation of a series of novel cycloamide-derived HIV-1 protease inhibitors. J Med Chem. 2005; 48:3576–3585. [PubMed: 15887965]
26. Chakraborti AK, Rudrawar S, Kondaskar A. Lithium bromide, an inexpensive and efficient catalyst for opening of epoxide rings by amines at room temperature under solvent-free condition. Eur J Org Chem. 2004; 2004:3597–3600.
27. Ghosh AK, Kincaid JF, Walters DE, Chen Y, Chaudhuri NC, Thompson WJ, Culberson C, Fitzgerald PMD, Lee HY, McKee SP, Munson PM, Duong TT, Darke PL, Zugay JA, Schleif WA, Axel MG, Lin J, Huff JR. Nonpeptidal P2 ligands for HIV protease inhibitors: structure-based

design, synthesis, and biological evaluation. J Med Chem. 1996; 39:3278–3290. [PubMed: 8765511]

28. Ghosh AK, Kincaid JF, Cho W, Walters DE, Krishnan K, Hussain JA, Koo Y, Cho H, Rudall C, Holland L, Buthod J. Potent HIV protease inhibitors incorporating high-affinity P2-ligands and (R)-(hydroxyethylamine)sulfonamide isostere. Bioorg Med Chem Lett. 1998; 8:687–690. [PubMed: 9871583]
29. Toth MV, Marshall GR. A simple, continuous fluorometric assay for HIV protease. Int J Pept Protein Res. 1990; 36:544–550. [PubMed: 2090647]
30. Tie Y, Boross PI, Wang YF, Gaddis L, Hussain AK, Leshchenko S, Ghosh AK, Louis JM, Harrison RW, Weber IT. High resolution crystal structures of HIV-1 protease with a potent non-peptide inhibitor (UIC-94017) active against multi-drug-resistant clinical strains. J Mol Biol. 2004; 338:341–352. [PubMed: 15066436]
31. Mahalingam B, Louis JM, Hung J, Harrison RW, Weber IT. Structural implications of drug-resistant mutants of HIV-1 protease: high-resolution crystal structures of the mutant protease/substrate analogue complexes. Proteins. 2001; 43:455–464. [PubMed: 11340661]
32. Otwinowski, Z., Minor, W. Processing of X-ray diffraction data collected in oscillation mode. In: Carter, CW., Jr, Sweet, RM., editors. Macromolecular Crystallography, Part A. Academic Press; Cambridge, MA: 1997. p. 307-326.
33. Shen CH, Wang YF, Kovalevsky AY, Harrison RW, Weber IT. Amprenavir complexes with HIV-1 protease and its drug resistant mutants altering hydrophobic clusters. FEBS J. 2010; 277:3699–3714. [PubMed: 20695887]
34. McCoy AJ, Grosse-Kunstleve RW, Adams PD, Winn MD, Storoni LC, Read RJ. Phaser crystallographic software. J Appl Crystallogr. 2007; 40:658–674. [PubMed: 19461840]
35. Winn MD, Ballard CC, Cowtan KD, Dodson EJ, Emsley P, Evans PR, Keegan RM, Krissinel EB, Leslie AGW, McCoy A, McNichols SJ, Murshudov GN, Pannu NS, Potterson EA, Powell HR, Read RJ, Vagin A, Wilson KS. Overview of the CCP4 suite and current developments. Acta Crystallogr Sect D: Biol Crystallogr. 2011; 67:235–242. [PubMed: 21460441]
36. Potterton E, Briggs P, Turkenburg M, Dodson E. A graphical user interface to the CCp4 program suite. Acta Crystallogr Sect D: Biol Crystallogr. 2003; 59:1131–1137. [PubMed: 12832755]
37. Sheldrick GM. A short history of SHELX. Acta Crystallogr Sect A: Found Crystallogr. 2008; 64:112–122.
38. Emsley P, Lohkamp B, Scott WG, Cowtan K. Features and development of Coot. Acta Crystallogr Sect D: Biol Crystallogr. 2010; 66:486–501. [PubMed: 20383002]
39. Schüttelkopf AW, van Aalten DMF. PRODRG: a tool for high-throughput crystallography of protein-ligand complexes. Acta Crystallogr Sect D: Biol Crystallogr. 2004; 60:1355–1363. [PubMed: 15272157]
40. Berman HM, Westbrook J, Feng Z, Gilliland G, Bhat TN, Weissig H, Shindyalov IN, Bourne PE. The protein data bank. Nucleic Acids Res. 2000; 28:235– 242. [PubMed: 10592235]

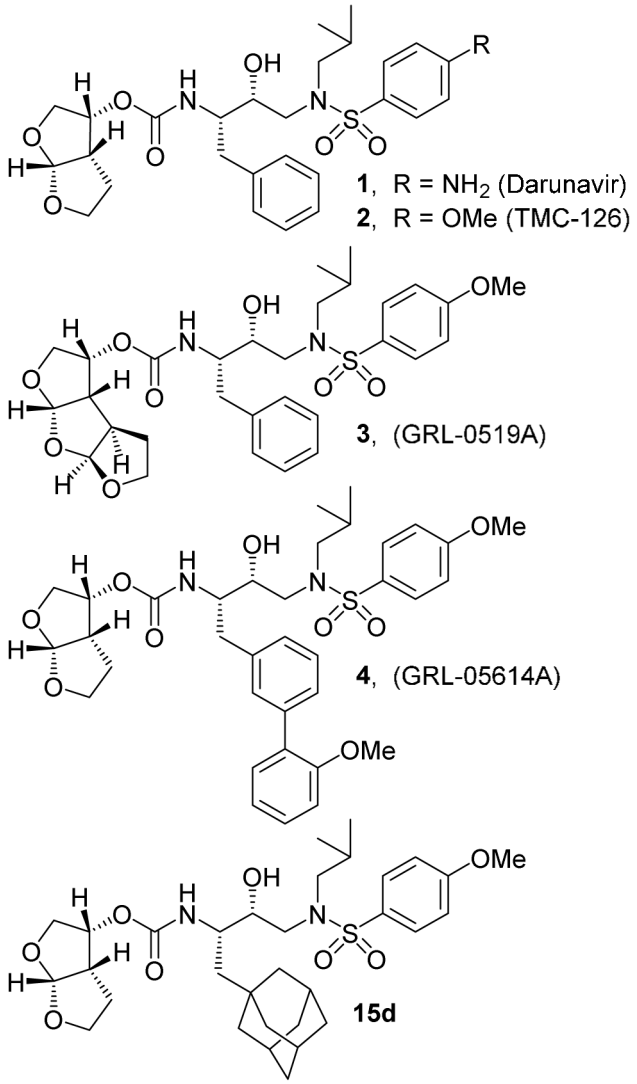

Figure 1.
Structure of PIs **1–4** and **15d**

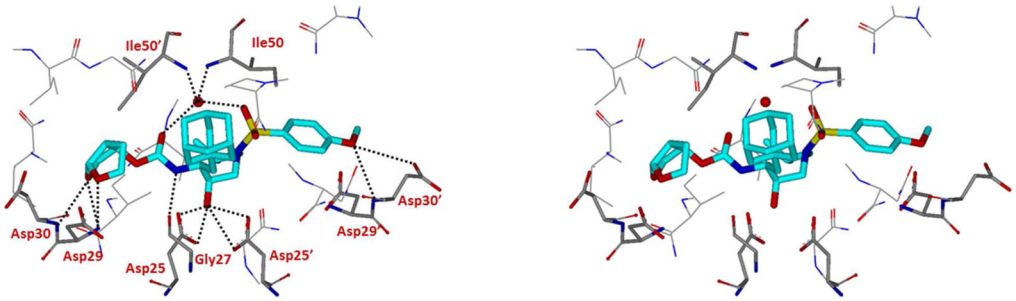

Figure 2.

Stereoview of the X-ray structure of inhibitor **15d** (turquoise color)-bound to the active site of wild-type HIV-1 protease (PDB code: 5JFP). All strong hydrogen bonding interactions are shown as black dotted lines.

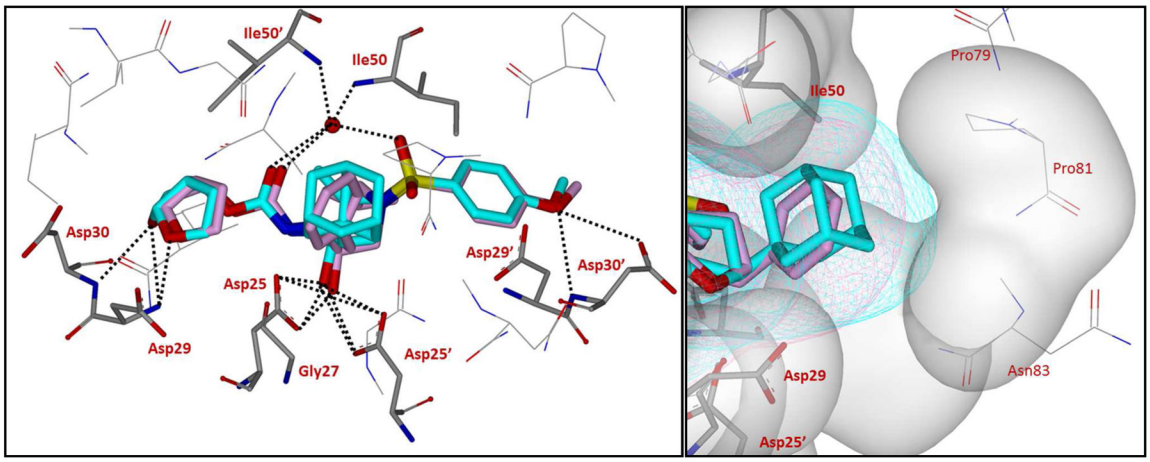

Figure 3.

Left: Overlay of TMC-126 (**2**) and **15d** in the HIV-1 protease active site. Right: Side view of the S1 subsite. Protein surface is shown in transparent gray, **2** surface is shown in pink wire mesh, and **15d** surface is shown in cyan wire mesh. Surfaces rendered using Accelrys DS ViewerPro.

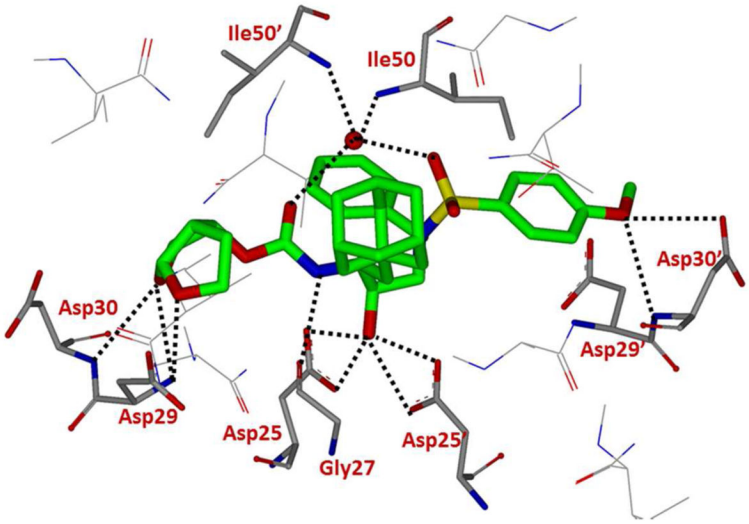

Figure 4.

X-ray structure of inhibitor **15h** (green) in the active site of wild-type HIV-1 protease (PDB: 5JFU). Relevant hydrogen bonds are shown as black dotted lines.

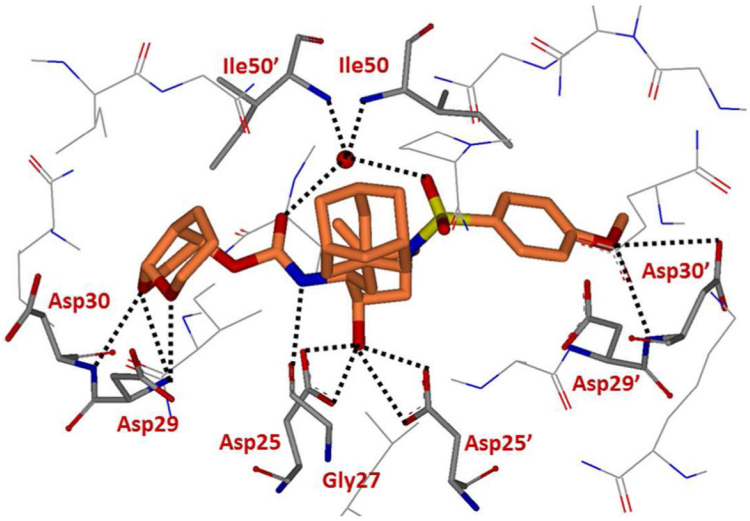

Figure 5.

X-ray structure of inhibitor **15i** (yellow) in the active site of wild-type HIV-1 protease (PDB: 5JG1). Relevant hydrogen bonds are shown as black dotted lines.

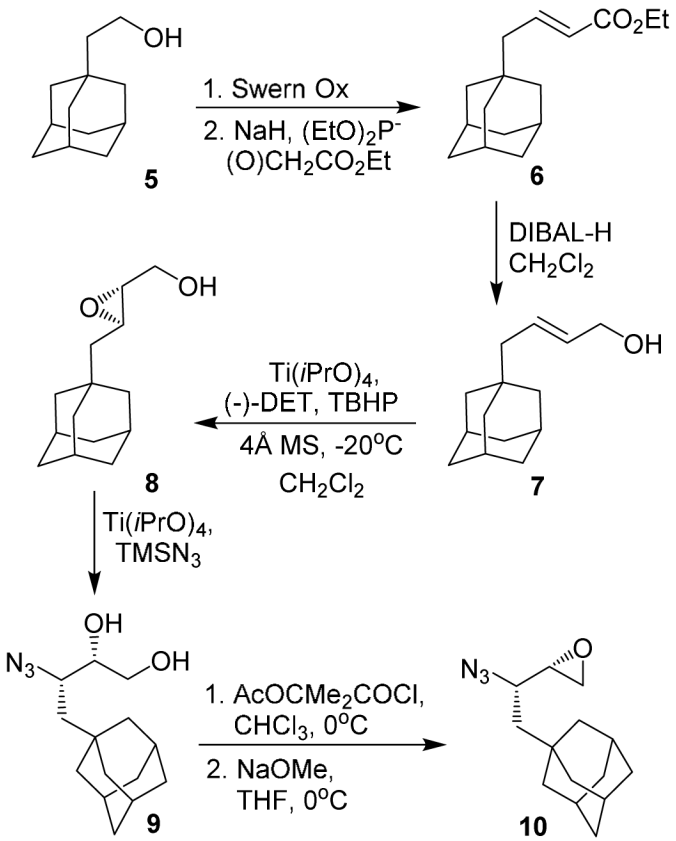

Scheme 1.
Synthesis of epoxide **10**

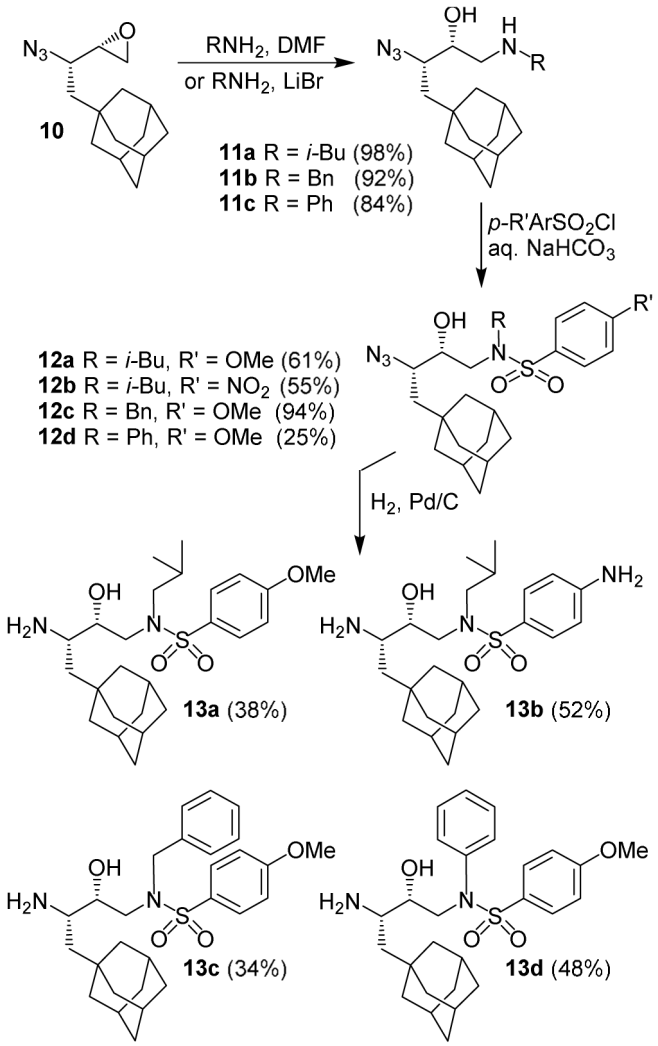

Scheme 2.
Synthesis of isosteres **13a–d**

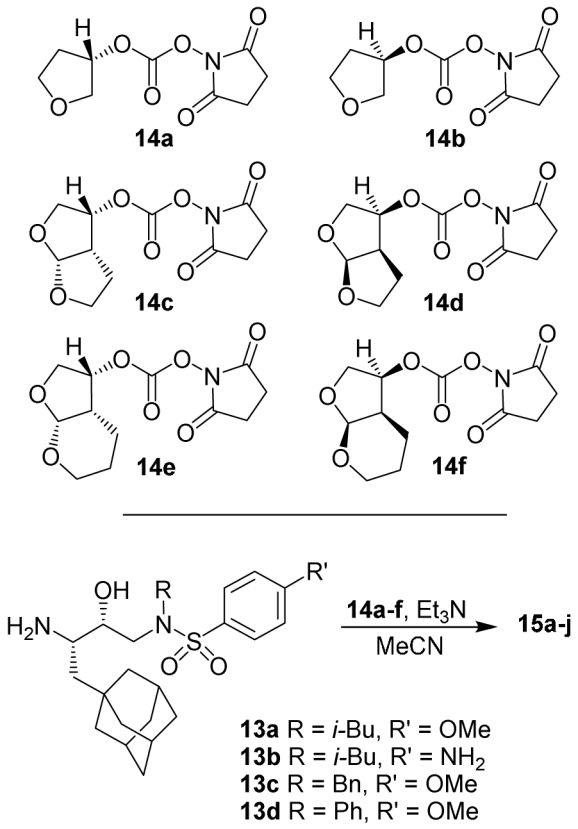

Scheme 3.

Synthesis of inhibitors **15a–j**

Table 1

Enzymatic inhibitory and antiviral activity of inhibitors

Entry	Inhibitor	K_i (nM)	IC_{50}(nM)[a,b]	Entry	Inhibitor	K_i (nM)	IC_{50}(nM)[a,b]
1.	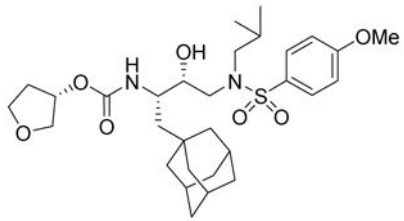 **15a**	0.54	39	6.	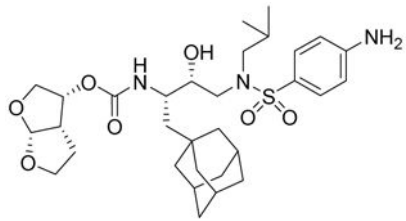 **15f**	0.73	60
2.	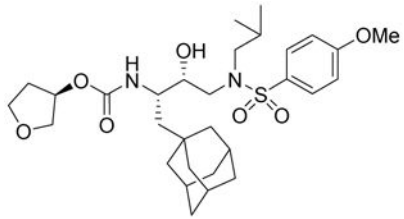 **15b**	2.8	nt	7.	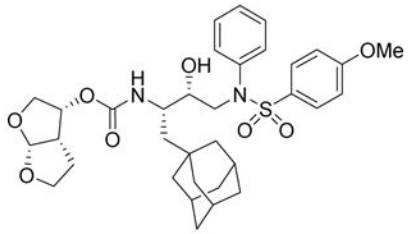 **15g**	1.1	nt
3.	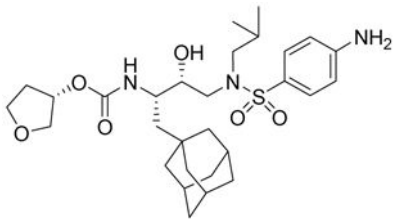 **15c**	3.4	580	8.	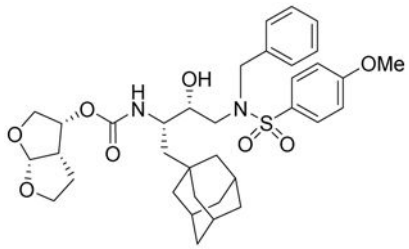 **15h**	8.5	310

Entry	Inhibitor	K_i (nM)	IC_{50}(nM)[a,b]	Entry	Inhibitor	K_i (nM)	IC_{50}(nM)[a,b]
4.	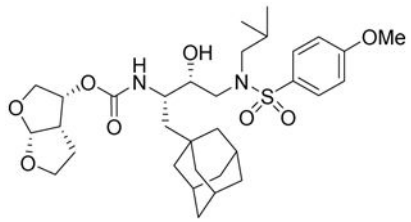 **15d**	0.48	32	9.	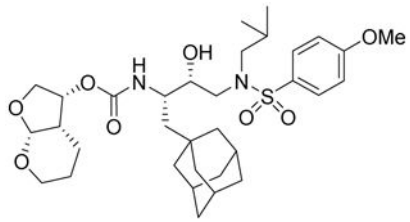 **15i**	1.9	460
5.	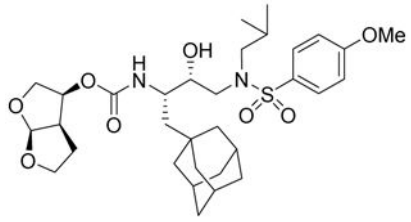 **15e**	1.0	nt	10.	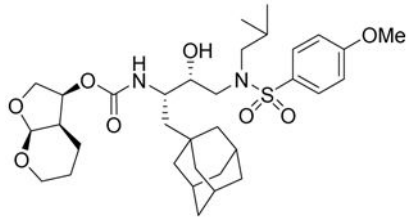 **15j**	24	>1000

[a] Human T-lymphoid (MT-2) cells were exposed to 100 $TCID_{50}$ values of HIV-1_{LAI} and cultured in the presence of each PI, and IC_{50} values were determined using the MTT assay. Darunavir exhibited K_i = 16 pM, IC_{50} = 3.0 nM.

[b] nt = not tested.

Table 2

Antiviral Activity of **15a** and **15d** against Multidrug Resistant HIV-1 Variants.

	Mean IC_{50} in TM ± SD [a,b]			
Compounds	**HIV-1_{NL4-3}**	**HIV-1_{B}**	**HIV-1_{C}**	**HIV-$1_{DRV}{}^{R}{}_{P20}$**
15a	0.46 ± 0.43	>1	>1	>1
15d	0.015 ± 0.008	>1	0.36 ± 0.06	>1
APV	0.017 ± 0.005	0.86 ± 0.21	0.43 ± 0.12	>1
DRV	0.0018 ± 0.0001	0.043 ± 0.002	0.03 ± 0.025	0.087 ± 0.061

[a] MT-4 cells (1×10^4) were exposed to 50 $TCID_{50}$s of wild-type HIV-1_{NL4-3} or a multi-drug resistant HIV-1 variant (HIV-1_{B}, HIV-1_{C}, or HIV-$1_{DRV}{}^{R}{}_{P20}$) and cultured in the presence of various concentrations of each compound, and the IC_{50} values were determined by the p24 assay. The amino acid substitutions identified in protease of HIV-1_{B}, HIV-1_{C}, and HIV-$1_{DRV}{}^{R}{}_{P20}$ compared to HIV-1_{NL4-3} include L10I/L33I/M36I/M46I/F53L/K55R/I62V/L63P/A71V/G73S/V82A/L90M/I93L,L10I/I15V/K20R/L24I/M36I/M46L/I54V/I62V/L63P/K70Q/V82A/L89M, and L10I/I15V/K20R/L24I/V32I/M36I/M46L/L63P/A71T/V82A/L89M, respectively.

[b] All assays were conducted in triplicate, and the data shown represent mean values (±1 standard deviation) derived from the results of two independent experiments.